

ATMOSPHERES OF PROTOPLANETARY CORES: CRITICAL MASS FOR NUCLEATED INSTABILITY.

R. R. RAFIKOV

IAS, Einstein Dr., Princeton, NJ 08540
Draft version October 31, 2018

ABSTRACT

Understanding atmospheres of protoplanetary cores is crucial for determining the conditions under which giant planets can form by nucleated instability. We systematically study quasi-static atmospheres of accreting protoplanetary cores for different opacity behaviors and realistic planetesimal accretion rates in various parts of protoplanetary nebula. We demonstrate that there are two important classes of atmospheres: (1) those having outer convective zone which smoothly merges with the surrounding nebular gas, and (2) those possessing almost isothermal outer radiative region which effectively decouples atmospheric interior from the nebula. A specific type of gaseous envelope which accumulates around a given core depends only on the relations between the Bondi radius of the core, photon mean free path in the nebular gas, and the luminosity radius (roughly the size of the sphere which can radiate accretion luminosity of the core at an effective temperature equal to the local nebular temperature). Cores in the inner parts of protoplanetary disk (within roughly 0.3 AU from the Sun) have large luminosity radii resulting in the atmospheres of the first type, while cores in the giant planet region (beyond several AU) have small luminosity radii and always accumulate massive atmospheres of the second type. Critical core mass needed for the nucleated instability to commence is found to vary considerably as a function of distance from the Sun. This mass is $5 - 20 M_{\oplus}$ at $0.1 - 1$ AU which is too large to permit the formation of “hot Jupiters” by nucleated instability near the cores that have grown in situ. In the region of giant planets critical core mass depends on the gas opacity and planetesimal accretion rate but is insensitive to the nebular temperature or density provided that the opacity in the outer radiative region does not depend on the gas density (e.g. dust opacity). This is true irrespective of whether the envelope’s interior is convective or radiative and numerical values of the critical core mass are similar in the two cases. Critical mass in the region of giant planets can be as high as $20 - 60 M_{\oplus}$ (for opacity $0.1 \text{ cm}^2 \text{ g}^{-1}$) if planetesimal accretion is fast enough for protoplanetary cores to form prior to the nebular gas dissipation. This might indicate that giant planets in the Solar System have gained massive gaseous atmospheres by nucleated instability only after their cores have accumulated most of the mass in solids during the epoch of oligarchic growth, subsequent to which planetesimal accretion slowed down and cores became supercritical.

Subject headings: planets and satellites: formation — solar system: formation — planetary systems: protoplanetary disks

1. INTRODUCTION.

Recent discoveries of Jupiter-like planets around other stars have boosted up efforts to understand the origin of giant planets, subject which has been under scrutiny since sixties (Safronov 1969; see Brush 1990 for a historical perspective). Currently one of the most popular and successful theories of giant planet formation is a core (or nucleated) instability hypothesis (Harris 1978; Mizuno et al. 1978). According to this idea massive hydrogen/helium atmospheres of planets like Jupiter and Saturn have been acquired as a result of unstable gas accretion onto a preexisting core made of rock and/or ice. Analytical arguments (Stevenson 1982; Wuchterl 1993) and numerical calculations (Mizuno 1980; Ikoma et al. 2000) suggest that the onset of core instability occurs when the mass of the gaseous atmosphere around the core becomes comparable to the core mass itself.

The following gedankenexperiment can help understand the nature of this instability: imagine placing a massive solid core into an infinite homogeneous gaseous medium. Gravitational pull from the core gives rise to a significant pressure perturbation near the core if the es-

cape speed from its surface is larger than the gas sound speed, see §2.2. On a short (dynamical) timescale gas settles into a pressure equilibrium configuration near the core. Since the thermal timescale is usually longer than the dynamical timescale, this gaseous envelope¹ initially has entropy equal to that of the gas in the surrounding nebula. Gas temperature at the core surface is rather high and this drives an outward transport of energy causing entropy of the envelope to decrease. As a result, gas density near the core goes up and envelope becomes more and more massive by slow accumulation (on a thermal timescale) of gas from the surrounding nebula.

Given enough time, atmosphere around the core that is not too massive cools down to the nebular temperature and becomes isothermal, acquiring large gaseous mass. Such atmosphere has exponential density profile with most of the mass concentrated near the core surface (Sasaki 1989). Cores are “not too massive” when the mass of this isothermal atmosphere is much smaller than the core mass. At the same time, exponential sensitivity to the core gravity (and mass) causes atmospheric mass to increase faster than the first power of the core

¹ We use terms “envelope” and “atmosphere” interchangeably.

mass. Because of that, different fate awaits gas around the core that is more massive: as the atmosphere cools down its mass at some point becomes comparable to the core mass and gas starts contributing significantly to the planetary gravity. Hydrostatic equilibrium cannot be established beyond this point, because accretion of more gas, which helps to reestablish pressure equilibrium, also acts now to increase the gravitational acceleration. As a result, instability commences allowing gas to accrete rapidly onto the core. Critical core mass at which instability becomes possible is thus set by the condition that the mass of the equilibrium atmosphere around the critical core is comparable to the core mass itself [apart from additional logarithmic factors intrinsic of the isothermal case, see Sasaki (1989)]. Note that if the core is very massive, or gas around it is very dense, then even the mass of the isentropic envelope forming around the core on the dynamical time after the core has been introduced into the nebula might exceed the core mass, making atmosphere unstable from the very start.

Real protoplanetary cores are not likely to be just passive solid bodies of constant mass. They accrete planetesimals and accretion not only increases the core mass with time but also leads to the release of substantial amount of energy at the surface of the core. This changes the steady state structure of the envelope which can no longer be purely isothermal (as it tends to become in the case of passive core). Even if we forget for a moment about the increase of the core mass caused by planetesimal accretion², luminosity coming from the core would cause temperature in a steady state atmosphere to be higher near the core surface than in the nebula. As a result, the gas at the same pressure is less dense around the radiating core than around passive one, meaning that the total atmospheric mass is *lower* for luminous core than for passive one. Nevertheless, similar to the isothermal case, the more massive the core is, the more massive is the envelope around it, and scaling between them is faster than linear. As a result, a concept of critical core mass holds again: stable equilibrium atmospheres cannot exist around the cores which are so massive that their atmospheric mass exceeds the core mass.

Previous numerical and analytical studies confirm this general picture of the core instability, but there are still some open issues. For example, Perri & Cameron (1974) and later Wuchterl (1993) have concluded that protoplanetary atmospheres are likely to be convective and that their interior structure and mass (which was found to be quite low) sensitively depend on the density and temperature of the gas in the surrounding nebula. Stevenson (1982) arrived at a very different conclusion by considering a simple analytical model of an atmosphere with a constant opacity. He found it to be radiative, massive, and its structure to be insensitive to the external conditions. His findings confirmed previous numerical results by Harris (1978), Mizuno et al. (1978), and Mizuno (1980).

The purpose of this study is to systematically explore the structure of atmospheres around accreting protoplanetary cores under a variety of conditions typical in the

² Energy release at the core surface might also come from radioactive decay or differentiation in the core which are not accompanied by the change in the core mass.

protoplanetary nebulae. Using analytically tractable but still realistic models we attempt to resolve the aforementioned issues concerning the state of the envelope. We try to single out physical parameters crucial for determining the atmospheric structure and this provides us with a general classification scheme of possible protoplanetary atmospheres. We are looking for the steady state structures under the explicit assumption that the mass of the gaseous envelope is smaller than the mass of the core which it surrounds. This restricts our quantitative results to cores with masses below critical mass, although all qualitative conclusions are valid even for critical cores and we use this to estimate the masses of critical cores, see §5.3.

We start by laying down the basics of the problem at hand — equations, important length and mass scales, boundary conditions — in §2. In §3 & 4 we derive solutions for two important classes of envelope structures typical in the region of giant and terrestrial planets. Envelope masses and critical core mass are calculated in §5. Our results and their implications are discussed in §6. Finally, we devote Appendices to technical issues which emerge in our calculations.

2. PROBLEM SETUP.

Throughout this study the following approximation to the protoplanetary disk structure [similar to the Minimum Mass Solar Nebula (MMSN)] is used:

$$\Sigma_g(a) \approx 100 \Sigma_p(a) \approx 3000 \text{ g cm}^{-2} a_1^{-3/2}, \quad (1)$$

$$T_0(a) \approx 300 \text{ K } a_1^{-1/2}, \quad (2)$$

where Σ_p, Σ_g are the particulate and gas surface densities correspondingly, T_0 is the gas temperature, and $a_n \equiv a/(n \text{ AU})$ is a distance from the Sun a scaled by $n \text{ AU}$. From (2) one can find the gas sound speed $c_0 \equiv (kT_0/\mu)^{1/2}$ (k is a Boltzmann constant and μ is a mean molecular weight) and gas density at the midplane $\rho_0 \equiv \Sigma_g \Omega / c_0$ [$\Omega \equiv (GM_\odot/a^3)^{1/2}$ is the orbital angular frequency, M_\odot is the Solar mass]:

$$c_0(a) \approx 10^5 \text{ cm s}^{-1} a_1^{-1/4}, \quad (3)$$

$$\rho_0(a) \approx 6 \times 10^{-9} \text{ g cm}^{-3} a_1^{-11/4}. \quad (4)$$

All numerical estimates in the text refer to this particular model of the protoplanetary disk.

2.1. Basic equations.

Our purpose is to calculate a spherically symmetric distribution of gas density ρ , pressure P , and temperature T around a solid core with the mass M_c embedded in the nebular gas. Spherical symmetry requires nebula to be at least roughly homogeneous around the core and we determine the conditions for this to be true in the next section. Structure of the static envelope as a function of distance r from the center of the core is governed by the equation of hydrostatic equilibrium:

$$\frac{\partial P}{\partial r} = -G \frac{M_c}{r^2} \rho. \quad (5)$$

where G is the gravitational constant and M_c is the mass of the core, which we take to be much larger than the mass of the gaseous envelope. Equation (5) is not applicable if envelope is rapidly rotating (when the azimuthal

velocity of gas is of the order of the local Keplerian velocity around the core), thus in the following discussion we assume envelope rotation to be slow.

Atmosphere is assumed to be heated from below by a source at the core surface with luminosity L . This energy can be transported by radiative diffusion or convection. We use the Schwarzschild criterion to determine the convective stability of the envelope:

$$\nabla < \nabla_{ad} \equiv \frac{\gamma - 1}{\gamma}, \quad \nabla \equiv \frac{\partial \ln T}{\partial \ln P}, \quad (6)$$

where ∇ is a temperature gradient, ∇_{ad} is its value under isentropic conditions. As usual, γ is a adiabatic index of the gas; for monoatomic gas $\nabla_{ad} = 2/5$, for diatomic (e.g. H_2) $\nabla_{ad} = 2/7$. Usage of the Schwarzschild criterion implies that envelope is chemically homogeneous and nonrotating — a more general Ledoux criterion should be used in the presence of the molecular weight gradient (Kippenhahn & Weigert 1990), and Høiland criterion has to be employed if envelope rotates rapidly (Tassoul 1978).

When atmosphere is convectively stable according to (6), energy released at the core surface has to be carried away radiatively. In this case one supplements (5) with the equation of radiation transfer. In the diffusion approximation, valid in the optically thick case, it reads

$$\frac{16\sigma T^3}{3\kappa\rho} \frac{\partial T}{\partial r} = -\frac{L}{4\pi r^2}, \quad (7)$$

where σ is a Stefan-Boltzmann constant and κ is the opacity. In the outer Solar System gas around the protoplanet can be so rarefied that the outer parts of the envelope are optically thin. This possibility is considered in more detail in §3.3.2.

Whenever the stability criterion (6) is violated energy in the envelope is transported by convection. In this study we assume that convection is so effective that the temperature gradient in the convective parts of the envelope is equal to the adiabatic temperature gradient ∇_{ad} . This is equivalent to supplementing (5) with adiabatic equation of state (isentropic gas)

$$P = K\rho^\gamma, \quad (8)$$

where K is the adiabatic constant — measure of the gas entropy. This approximation should be good enough in the dense regions of the envelope (very good in the interiors of present day giant planets). In Appendix D we determine under what circumstances this zero entropy gradient assumption is valid in the atmospheres of protoplanetary cores.

We suppose the luminosity L to be derived from the accretion of planetesimals and neglect the additional energy release due to the radioactive heating and differentiation inside the core. Thus we take

$$L = G \frac{M_c \dot{M}}{R_c}, \quad (9)$$

where \dot{M} is a planetesimal accretion rate. In Appendix A we briefly summarize three different regimes of planetesimal accretion important for the core growth, and calculate \dot{M} and accretion timescale for each of them. Equation (9) assumes that (a) planetesimal velocity at infinity relative to the core is not too large compared to the core's escape speed, and (b) planetesimals penetrate

to the core surface without much resistance from the envelope and release there all their kinetic energy. First assumption is quite reasonable during the buildup of the core by planetesimal accretion; second should be valid for large planetesimals but small ones may be slowed down by the gas drag in the envelope as they make their way to the core surface. In the latter case accretion energy release does not occur exactly at the core surface but is distributed throughout the envelope, meaning that luminosity depends on r . However, even in the most unfavorable case of small planetesimals which are quasi-statically lowered from the top of the atmosphere to its bottom, luminosity is $(1 - R_c/r)L$, where R_c is the core radius, i.e. luminosity is not constant only very near the core's surface (Pollack et al. 1996). Beyond several R_c , in the bulk of the envelope, we can still safely assume that L is constant and given by (9).

Use of the steady state equations (5) and (7) tacitly assumes that envelope can quickly adjust to the changes in the core mass M_c and luminosity L caused by the planetesimal accretion. In other words, these equations hold only provided that the dynamical and thermal timescales of the envelope are shorter than the core accretion timescale, and we demonstrate in Appendix C that this assumption is reasonable. We also show there that in the framework of quasi-stationary approximation energy release within the envelope due to gas accretion can be naturally neglected compared to the planetesimal accretion luminosity (9).

2.2. Important length scales.

There are several characteristic length scales which are important for the problem at hand. One of them is the so-called Hill radius $r = R_H$ defined by

$$R_H \equiv a \left(\frac{M_c}{M_\odot} \right)^{1/3} \approx 2 \times 10^{11} \text{ cm } a_1 \left(\frac{M_c}{M_\oplus} \right)^{1/3}, \quad (10)$$

Fluid elements at about R_H from the protoplanetary core are equally affected by the core gravity and the tidal field of the central star. Within the Hill sphere gas dynamics is determined by the gravity of the core, while outside of it gas is subject mostly to the stellar gravity.

Physical size of the core R_c scales with M_c in the same way as R_H does, meaning that their ratio p is a constant depending only on the physical density of the protoplanet ρ_c and the core location in the protoplanetary disk:

$$p \equiv \frac{R_c}{R_H} = \left(\frac{3}{4\pi} \frac{M_\odot}{\rho_c a^3} \right)^{1/3} \approx 5.2 \times 10^{-3} a_1^{-1} \rho_1^{-1/3} \quad (11)$$

where $\rho_1 \equiv \rho/(1 \text{ g cm}^{-3})$. One can easily see that $R_c \ll R_H$.

Bondi radius R_B is defined as the distance from the protoplanet at which the thermal energy of the nebular gas is of the order of its gravitational energy in the potential well of the core:

$$R_B \equiv G \frac{M_c}{c_0^2} \approx 4 \times 10^{10} \text{ cm } a_1^{1/2} \frac{M_c}{M_\oplus}. \quad (12)$$

Outside Bondi sphere ($r \gtrsim R_B$) gravity of the core is too weak to strongly affect the gas; consequently, gas pressure is almost equal to its nebular value P_0 . Inside Bondi sphere pressure is significantly perturbed by the protoplanetary gravity.

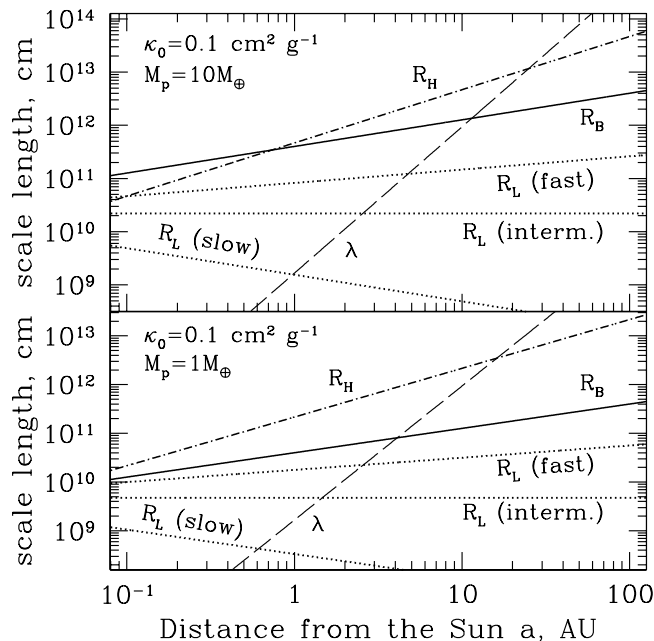


FIG. 1.— Different length scales important for atmospheric structure as a function of semi-major axis a for $\kappa_0 = 0.1 \text{ cm}^2 \text{ g}^{-1}$ and two values of core mass: $M_c = 10 M_\oplus$ (*top*) and $M_c = 1 M_\oplus$ (*bottom*). Solid, dashed, and dot-dashed lines represent R_B , λ , and R_H correspondingly. Dotted lines correspond to luminosity radius R_L evaluated for three different planetesimal accretion regimes — fast, intermediate, and slow (see Appendix A) — labeled on the plot. The meaning of other curves is clear from the corresponding labels.

Opacity of the gas sets another important scale. We consider a rather general opacity law by assuming throughout this work that

$$\kappa = \kappa_0 (P/P_0)^\alpha (T/T_0)^\beta. \quad (13)$$

Previous studies (Mizuno 1980; Stevenson 1982) have always assumed dust opacity in the outer layers of the envelope assuming it to be constant. At the same time, opacity due to small interstellar dust grains (smaller than the typical wavelength of the local blackbody radiation) is thought to behave as $\kappa \propto T^\beta$ (i.e. $\alpha = 0$) with $\beta \approx 1 - 2$ (Draine 2003) in the range of temperatures typical for protoplanetary disks (although this is a statement depending on the size distribution and composition of the dust, which in the protoplanetary disks can be different from those in the ISM). Our opacity prescription (13) accounts for this possibility and is more general compared to the previous treatments. Opacity in the inner layers of the envelope (likely dominated by the molecular opacity of H_2 and H_2O for which one has to use opacity tables) might not be so important for the envelope structure or mass — atmosphere can be convective there, see §6.1. Opacity effects are quantified by introducing a mean absorption length of photons in the nebular gas

$$\lambda \equiv (\kappa_0 \rho_0)^{-1} \approx 1.7 \times 10^9 \text{ cm } a_1^{11/4} \left(\frac{0.1 \text{ cm}^2 \text{ g}^{-1}}{\kappa_0} \right) \quad (14)$$

The exact value of κ_0 is highly uncertain because the amount of dust and its size distribution in protoplanetary disks are poorly constrained. Thus, we treat κ_0 as a parameter and for simplicity take it to be constant

throughout the nebula, independent of a . Outer parts of the protoplanetary nebula are optically thin, meaning that λ is larger than the vertical disk scale height $h \equiv c_0/\Omega$.

Finally, luminosity of the core sets one more length scale

$$R_L \equiv \left(\frac{L}{16\pi\sigma T_0^4} \right)^{1/2}, \quad (15)$$

which is a size of object radiating luminosity L at an effective temperature T_0 . In Figure 1 we plot R_L together with other length scales as a function of a for two values of κ_0 and for different accretion regimes (see Appendix A).

Nebula can be considered homogeneous on the scale of R_B only if R_B is small compared to the disk scaleheight h . This condition puts the following constraint on the mass of the core:

$$M_c \ll M_1 \equiv \frac{c_0^3}{G\Omega} \approx 12 M_\oplus a_1^{3/4}. \quad (16)$$

Whenever this condition is fulfilled the Bondi radius is also smaller than R_H , while R_H is smaller than h , see equation (17). For $M_c \gg M_1$ Bondi radius lies outside R_H and nebular gas in the Hill sphere is very inhomogeneous ($R_H \gg h$) and strongly perturbed by the protoplanetary gravity. At 10 AU (16) constrains M_c to be less than $\approx 70 M_\oplus$, while at 30 AU $M_1 \approx 150 M_\oplus$. Note that (16) is also an approximate condition for the absence of strong spatial gradients in the nebula caused by the dissipation of the core-induced density waves (Lin & Papaloizou 1993; Rafikov 2002). As a result, one does not have to worry about the gap formation.

With the use of (16) one can rewrite (12) in the following form:

$$R_B = R_H \left(\frac{M_c}{M_1} \right)^{2/3} = R_c \left(\frac{M_c}{M_2} \right)^{2/3}, \quad (17)$$

where

$$M_2 \equiv p^{3/2} M_1 \approx 4.5 \times 10^{-3} M_\oplus a_1^{-3/4} \rho_1^{-1/2} \quad (18)$$

is another fiducial mass scale. If the core mass M_c is smaller than M_2 then $R_B \lesssim R_c$, meaning that the protoplanet is too small to induce appreciable pressure perturbations in the surrounding gas even at its surface and thus has no atmosphere associated with it. We will study only the cores satisfying

$$M_2 \ll M_c \ll M_1 \quad (19)$$

since they are massive enough to possess atmospheres and small enough for the surrounding gas to be thought of as roughly homogeneous on the scale of R_B , i.e. $R_c \ll R_B \ll R_H \ll h$. One can see that the mass range in which (19) is valid is rather large and spans 4 – 5 orders of magnitude depending on a (e.g. from ~ 0.1 Lunar mass to $\sim M_J$ at 10 AU). In Figure 2 we demonstrate how the different length scales are related to each other as a function of a and M_c/M_1 , constrained by (19).

2.3. Boundary conditions.

Boundary conditions to the equations of §2.1 specify that gas pressure, temperature, and density should

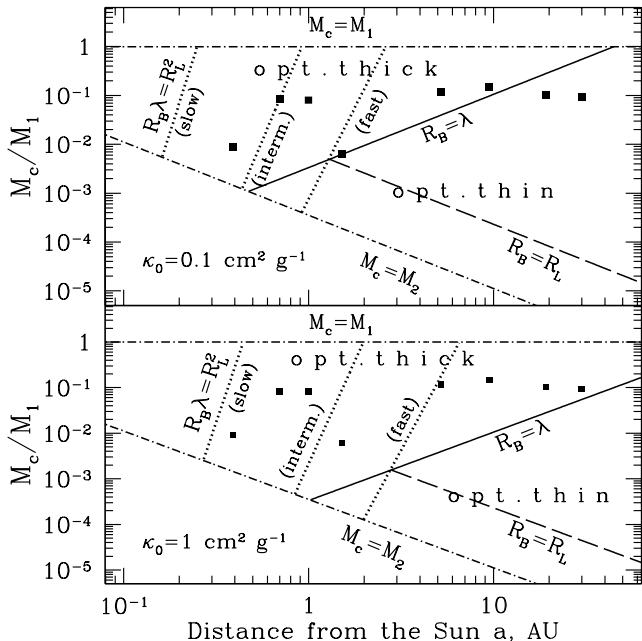


FIG. 2.— Relationships between different length scales as a function of semi-major axis a in the nebula for two values of gas opacity (assumed constant throughout the nebula): $\kappa_0 = 0.1 \text{ cm}^2 \text{ g}^{-1}$ (top) and $\kappa_0 = 1 \text{ cm}^2 \text{ g}^{-1}$ (bottom). Only the case $M_2 < M_c < M_1$ is considered (dot-dashed boundaries). Dotted lines correspond to condition $R_B \lambda = R_L^2$ for three different planetesimal accretion regimes labeled on the curves. Solid line represents $R_B = \lambda$ separating optically thick and optically thin regimes (see §3.1 and 3.2), while dashed line is for $R_B = R_L$. Squares mark positions of 8 major planets of the Solar System on this diagram; for Jupiter and Saturn we assume cores of $5 M_\oplus$ and $10 M_\oplus$.

reduce to their nebular values P_0 , T_0 , and ρ_0 at some distance R_{out} from the core:

$$T(R_{out}) = T_0, \quad P(R_{out}) = P_0, \quad \rho(R_{out}) = \rho_0. \quad (20)$$

The problem then is to determine the value of R_{out} .

The most simplistic way of evaluating R_{out} would be to completely neglect the fact that the nebula surrounding the core is in the differential motion caused by the gravity of the central star. If one does this and assumes gas to be static everywhere, then R_{out} can be set equal to infinity. Presence of the shearing motion in the nebula drastically changes the dynamical and thermal behavior of the gas in the core's vicinity. First, gas inside the Hill sphere moves in a rather complicated way as demonstrated by the hydrodynamical simulations of planet-disk interaction (e.g. D'Angelo et al. 2002, 2003); but we can hope that this will not violate our assumption of nebula homogeneity in the core vicinity if $R_B \lesssim R_H$ (or $M_c \lesssim M_1$).

Second, the flow of the nebular gas within the Hill sphere can effectively “cool” the outer part of the envelope by advecting the gas heated by the core's accretional energy release away from the core and bringing in fresh gas having entropy equal to the nebular entropy. This process should determine the value of R_{out} at which temperature drops to T_0 . Apparently, $R_{out} \gtrsim R_B$ since gas within Bondi sphere is confined by the core's gravity and is not being refreshed. At the same time, the distance from the core center at which the boundary condition for the pressure is imposed is determined by a different process — dominance of the core gravity over the thermal

pressure in the nebula (and, possibly, over the centrifugal forces induced by the fluid motion around the gravitationally bound part of the envelope which we neglect in this study). Apparently, pressure may converge to P_0 only beyond R_B ; thus, we again arrive at the restriction $R_{out} \gtrsim R_B$ but now from the point of view of pressure balance.

A proper estimate of distance R_{out} at which the thermal and pressure boundary conditions are imposed must include inhomogeneous heating within R_{out} , geometry of the flow near the core, vertical structure of the nebula, possibility of formation of rotationally supported disk around the core, and so on. This is beyond the scope of this study. Fortunately, it turns out (see §6.3) that the exact value of R_{out} is not important for the envelope structure as long as $R_{out} \gg R_B$ (we checked this to be true); in our calculations we simply set $R_{out} = 20R_B$.

3. ATMOSPHERES WITH OUTER RADIATIVE ZONE.

Relationships between the various length scales defined in §2.2 are quite different in the inner and outer parts of the nebula. As Figure 2 demonstrates, for protoplanetary cores with $M_c \approx (1-10)M_\oplus$ accreting planetesimals in the fast regime at $a \gtrsim (2-5)$ AU, one of the two sets of inequalities

$$\lambda \ll R_B, \quad R_L^2 \ll \lambda R_B, \quad \text{or} \quad (21)$$

$$R_L \ll R_B \ll \lambda, \quad (22)$$

is typically fulfilled depending on a and κ_0 . This is mainly because the planetesimal accretion rate \dot{M} and nebular gas density ρ_0 decrease with a reducing R_L and increasing λ . For smaller cores or slower accretion regime these conditions can hold even closer to the Sun. We demonstrate later on that when either (21) or (22) is valid, there exists an almost isothermal radiative layer in the outer part of the envelope which decouples its interior from the nebular gas. Although the structure of this layer is slightly different in two cases, properties of the inner envelope will be shown to be universal.

3.1. Low luminosity, optically thick ($\lambda \lesssim R_B$ and $R_L^2 \ll \lambda R_B$).

Whenever the photon mean-free path λ is shorter than the Bondi radius R_B , envelope is optically thick to the escaping radiation. In this case its structure is completely determined by equations (5) and (7). Integrating them together with (13) and using boundary condition $P = P_0$ when $T = T_0$ (at $r = R_{out}$, see [20]) one finds that

$$\left(\frac{P}{P_0}\right)^{1+\alpha} - 1 = \frac{4\nabla_0 R_B \lambda}{3 R_L^2} \left[\left(\frac{T}{T_0}\right)^{4-\beta} - 1 \right],$$

$$\nabla_0 \equiv \frac{1+\alpha}{4-\beta} \quad (23)$$

Constant ∇_0 is positive whenever T increases with depth; we assume this to be the case which requires $\beta < 4$ since normally opacity does not decrease with increasing density (i.e. $\alpha \geq 0$). The meaning of ∇_0 will become clear later on (see §3.3). The coefficient in the right hand side of (23) is very large because of (21), so that a large change of pressure results in only a small perturbation of temperature.

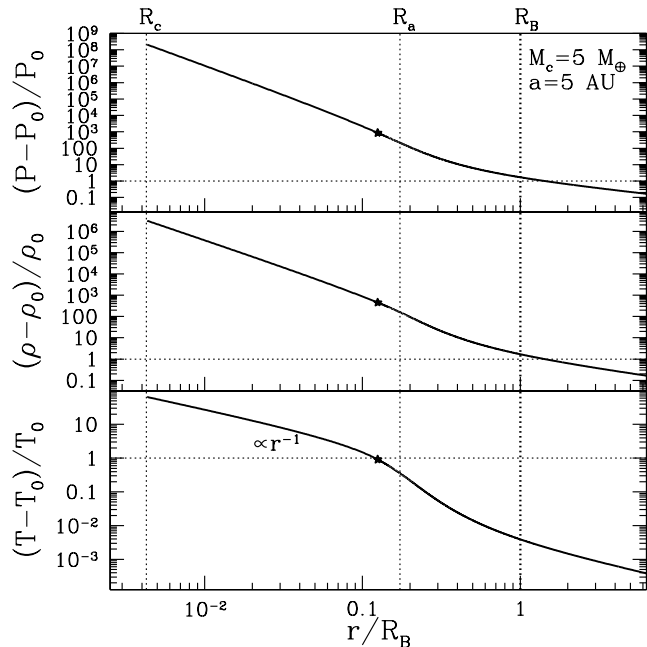


FIG. 3.— Atmospheric structure around the core with $M_c = 5 M_\oplus$ at 5 AU. Relative deviations of P , ρ , and T from their nebular values calculated numerically are shown ($P_0 = 3.2 \times 10^{-7}$ bar, $\rho_0 = 7 \times 10^{-11}$ g cm $^{-3}$ and $T_0 = 130$ K in the surrounding nebula). Calculation is done for $\alpha = 0$, $\beta = 1$, $\gamma = 7/5$ and $\kappa = 0.1$ cm 2 g $^{-1}$. In this particular case $\lambda < R_B$ and $R_B \lambda / R_L^2 \approx 300$, i.e. envelope is optically thick everywhere and has an outer radiative zone, see §3.3.1. Stars mark the position of the outer edge of the inner convective region.

To make further progress we need to substitute (23) into either (5) or (7) and find the P and T dependencies on r . This can be done numerically for arbitrary α and β . Here we look at the asymptotic behavior of the envelope properties in two limiting cases: in the outer atmosphere where $T - T_0 \lesssim T_0$, and deep in the envelope where $T \gg T_0$.

In the first case envelope is essentially isothermal; solving (5) under this assumption one obtains

$$P/P_0 = \rho/\rho_0 = \exp\left(\frac{R_B}{r} - \frac{R_B}{R_{out}}\right). \quad (24)$$

Temperature profile can then be simply obtained from (23) as

$$\frac{T - T_0}{T_0} \approx \frac{3}{4(1 + \alpha)} \frac{R_L^2}{R_B \lambda} \times \left\{ \exp\left[(1 + \alpha) \left(\frac{R_B}{r} - \frac{R_B}{R_{out}}\right)\right] - 1 \right\}, \quad (25)$$

where boundary conditions (20) were again used. One can see from (25) that temperature perturbation at $r \sim R_B$ is small because $R_B \lambda / R_L^2 \gg 1$; at the same time gas density and pressure within Bondi sphere grow exponentially, see (24). Gas temperature rises to several times T_0 only when the distance to the core center becomes as small as

$$R_a \equiv R_B \frac{1 + \alpha}{\ln(R_B \lambda / R_L^2)}. \quad (26)$$

Apparently, $R_a \ll R_B$ although one should keep in mind

that R_a depends on $R_B \lambda / R_L^2$ only logarithmically. Pressure P_a and density ρ_a at this depth are

$$P_a/P_0 \approx \rho_a/\rho_0 \approx (R_B \lambda / R_L^2)^{1/(1+\alpha)} \gg 1. \quad (27)$$

Existence of the outer radiative layer, in which temperature is almost constant while density dramatically increases was first found numerically by Harris (1978) under the conditions typical in the region of giant planets. Note that the presence of the outer isothermal layer does not necessarily require gas to be optically thin, cf. Mizuno et al. (1978).

In a second limiting case, interior to R_a , we use $T \gg T_0$ to integrate (7) with (23). Using $T \approx \xi T_0$ ($\xi \sim 1$) at $r = R_a$ as an approximate boundary condition at the transition point one finds that

$$\frac{T}{T_0} \approx \xi + \nabla_0 \left(\frac{R_B}{r} - \frac{R_B}{R_a} \right), \quad (28)$$

$$\frac{P}{P_0} \approx \left(\frac{4 \nabla_0 \lambda R_B}{3 R_L^2} \right)^{1/(1+\alpha)} \left[\xi + \nabla_0 \left(\frac{R_B}{r} - \frac{R_B}{R_a} \right) \right]^{1/\nabla_0} \quad (29)$$

In the case of constant opacity ($\alpha = \beta = 0$, $\nabla_0 = 1/4$) this solution reduces to the radiative zero solution found by Stevenson (1982) for $r \ll R_a$. Figure 3 shows the internal structure of the atmosphere around $5 M_\oplus$ core at 5 AU (for which [21] is valid) calculated using (5) and (23). Opacity with $\alpha = 0$, $\beta = 1$ and $\kappa_0 = 0.1$ cm 2 g $^{-1}$ as well as $\gamma = 7/5$ are assumed in calculation. This specific scaling of κ with P and T makes the inner part of the envelope convective below R_a (see §3.3), but this hardly changes the overall picture of the atmospheric structure that we described in this section.

3.2. Low luminosity, optically thin ($R_L \ll R_B \lesssim \lambda$).

Whenever $\lambda \gtrsim R_B$ there is an optically thin region around the protoplanet in which the photon mean free path is larger than the length scale over which physical variables such as pressure and temperature experience significant changes. Deep in the envelope (below the photosphere) optical depth increases and atmosphere becomes optically thick. Gas is optically thick also far from the core since the density and temperature scale height is $\sim r$ there and the optical depth to radiation escaping from the core becomes larger than unity at $r \gtrsim \lambda$. Of course, this outer optically thick region can only exist if $\lambda \lesssim h$ and nebula is homogeneous on scales $\sim \lambda$, which is not the case in the outer parts of protoplanetary disks (but this turns out not to be important). Thus, the optically thin zone around the core in the infinite medium should be sandwiched between the inner and outer optically thick regions.

Temperature structure in the optically thick parts is determined by equation (7). In the optically thin region we have $T^4 \approx T_0^4 + L/(16\pi\sigma r^2)$, where the additional factor of 4 in the denominator of the second term comes from the anisotropy of the core radiation. Similar behavior of T in the optically thin region was found by Hayashi et al. (1979). Strictly speaking, this expression is accurate only far from the photosphere and we should expect it to reproduce photospheric temperature only approximately (which will not affect our results in any significant way). Thus, we express envelope temperature

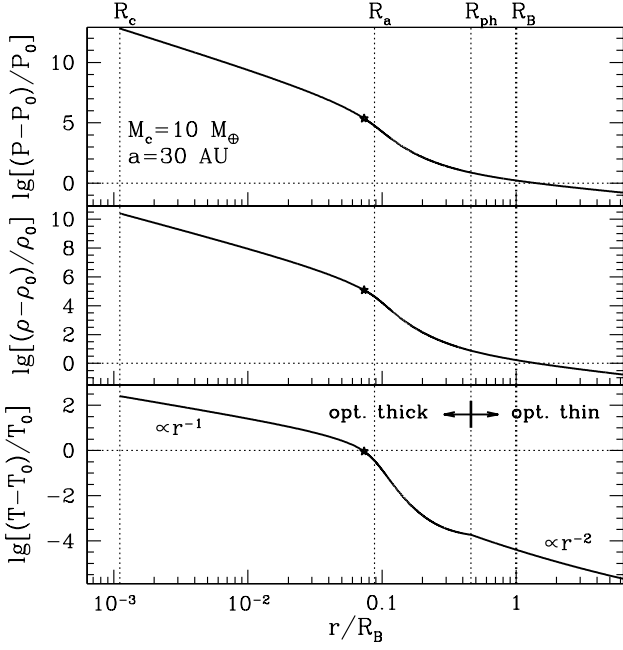


FIG. 4.— Same as Figure 3 but for $M_c = 10 M_\oplus$ at 30 AU. In this particular case $P_0 = 10^{-9}$ bar, $\rho_0 = 5 \times 10^{-13}$ g cm $^{-3}$ and $T_0 = 55$ K. Also $\lambda > R_B$ and $R_B \lambda / R_L^2 \approx 10^5$, i.e. envelope has an outer optically thin region and possesses an outer radiative zone, see §3.3.2. The rest of notation is as in Figure 3.

profile above the photosphere as

$$T^4(r) \approx T_0^4 + \frac{L}{16\pi\sigma r^2} + \frac{3L}{16\pi\sigma} \int_r^\infty \frac{\kappa\rho(r')dr'}{r'^2} \quad (30)$$

The second term on the right hand side is relevant for the optically thin region while the third becomes important outside of $r \approx \lambda$ where photons couple to the nebular gas and start to diffuse.

Gas pressure is close to P_0 for $r \gtrsim R_B$. Assuming that $T - T_0 \ll T_0$ everywhere in this region we have $\rho \approx \rho_0$ and $\kappa \approx \kappa_0$. Then it follows from (30) that

$$T(r) \approx T_0 \left[1 + \frac{R_L^2}{r^2} + 3 \frac{R_L^2}{\lambda r} \right]^{1/4}. \quad (31)$$

It is very important that the temperature perturbation at the Bondi sphere $T(R_B) - T_0 \sim T_0 (R_L/R_B)^2$ is negligible whenever (22) is fulfilled (similar to the optically thick case considered in §3.3.1) — this verifies our assumption of $T \approx T_0$ for $r \gtrsim R_B$. This result is independent of whether λ is larger or smaller than h or R_H , what is crucial is that $R_L \ll R_B \ll \lambda$ (which makes third term in [31] negligible compared to the second at $r \sim R_B$). Temperature deviation $T - T_0$ is dominated by the radiative diffusion for $r \gtrsim \lambda$ (third term in brackets) and by the optically thin radiation transfer for $r \lesssim \lambda$.

Inside the Bondi sphere gas is initially still optically thin and its temperature is determined by (31) meaning that $T \approx T_0$. At the same time, pressure and density in this essentially isothermal region increase exponentially with depth in accordance with (24). As a result, local photon mean free path rapidly decreases and envelope finally becomes optically thick to the escaping radiation. Photosphere is located at the distance R_{ph} from the core

center where the photon mean free path becomes comparable to the typical length scale of density variation. Using (24) we estimate that the density scale height is $\partial r / \partial \ln \rho = r^2 / R_B$, which becomes comparable to $(\kappa\rho)^{-1}$ at

$$R_{ph} \approx R_B \frac{1 + \alpha}{\ln(\lambda/R_B)}, \quad (32)$$

whenever $R_B \ll \lambda$. We find from (31) that gas temperature at the photosphere $T_{ph} \equiv T(R_{ph})$ is offset from T_0 by

$$\frac{T_{ph} - T_0}{T_0} \approx \frac{R_L^2}{4R_{ph}^2} \approx \left[\frac{\ln(\lambda/R_B) R_L}{2(1 + \alpha) R_B} \right]^2 \ll 1, \quad (33)$$

while the photospheric pressure $P_{ph} \equiv P(R_{ph})$ is

$$P_{ph}/P_0 \approx (\lambda/R_B)^{1/(1+\alpha)} \gg 1. \quad (34)$$

We see that T_{ph} is still only slightly different from T_0 , while the photospheric pressure is much higher than P_0 if (22) holds.

Below the photosphere, we again resort to equations (5) and (7). Similar to (23) one finds for boundary conditions $P = P_{ph}$ at $T = T_{ph}$ that

$$\begin{aligned} & \left(\frac{P}{P_0} \right)^{1+\alpha} - \left(\frac{P_{ph}}{P_0} \right)^{1+\alpha} \\ &= \frac{4\nabla_0 R_B \lambda}{3 R_L^2} \left[\left(\frac{T}{T_0} \right)^{4-\beta} - \left(\frac{T_{ph}}{T_0} \right)^{4-\beta} \right]. \end{aligned} \quad (35)$$

When $|T - T_0|/T_0 \lesssim 1$ we can still use (24) for the density profile; then the temperature profile for $r \lesssim R_{ph}$ derived from (35) becomes

$$\begin{aligned} \frac{T - T_{ph}}{T_0} &\approx \frac{3}{4(1 + \alpha)} \frac{R_L^2}{R_B \lambda} \\ &\times \left\{ \exp \left[\left(1 + \alpha \right) \frac{R_B}{r} \right] - (P_{ph}/P_0)^{1+\alpha} \right\}, \end{aligned} \quad (36)$$

where we took into account that $R_B/R_{out} \lesssim 1$. Keeping in mind that according to (22) and (34) $(P_{ph}/P_0)^{1+\alpha} \ll R_B \lambda / R_L^2$, one easily finds that the distance R_a at which gas temperature starts to appreciably deviate from T_0 is still given by (26). Thus, under conditions (22) R_a is still located deep inside the envelope, and always below the photosphere, compare with (32).

It is also easy to deduce from (35) that for $r \lesssim R_a$ temperature and pressure behavior in the inner envelope are still described by equations (28) and (29). Thus, despite the differences in the structure of the outer atmosphere ($r \gtrsim R_a$) in the optically thin ($R_L \ll R_B \ll \lambda$) and optically thick ($\lambda \ll R_B$, $R_L^2 \ll \lambda R_B$) cases, the structure of the inner atmosphere is the same. In Figure 4 properties of the envelope around $10 M_\oplus$ core at 30 AU (for which [22] is valid) are exhibited. Temperature profile in the optically thin region was calculated using (30), and all parameters (opacity, value of γ) are the same as those used for Figure 3, see §3.3.1.

3.3. Convective stability.

In §3.3.1-3.3.2 we have assumed that energy transfer from the bottom to the top of the atmosphere occurs by radiative transport. Here we explicitly determine under

which circumstances this is the case, and also calculate envelope structure in convectively unstable regions.

To check our solutions obtained in previous sections for convective stability we calculate ∇ and use the Schwarzschild criterion (6). It turns out that the outer part of the envelope above R_a is stable whenever (21) or (22) is fulfilled. Indeed, in the optically thick case (see §3.3.1) we find using (5), (7), and (23) that

$$\begin{aligned} \nabla(T) &= \frac{3}{4} \frac{R_L^2}{R_B \lambda} \left(\frac{T}{T_0} \right)^{\beta-4} \left(\frac{P}{P_0} \right)^{1+\alpha} \\ &= \nabla_0 \left\{ 1 - \left(\frac{T_0}{T} \right)^{4-\beta} \left[1 - \frac{3}{4\nabla_0} \frac{R_L^2}{R_B \lambda} \right] \right\}. \end{aligned} \quad (37)$$

Because of the limitations imposed by (21) this reduces to

$$\nabla \approx \nabla_0 \left[1 - \left(\frac{T_0}{T} \right)^{4-\beta} \right], \quad (38)$$

[relative corrections to this expression are at the most $O(R_L^2/R_B \lambda) \ll 1$]. Thus, outside of R_a , where $T \approx T_0$, temperature gradient is small and atmosphere is convectively stable. We also see from (38) that ∇_0 has a meaning of temperature gradient deep inside the radiative envelope where $T \gg T_0$.

In the optically thin case (see §3.3.2) one finds similar situation. Temperature above the photosphere is almost equal to T_0 (see equations [31] and [33]) while pressure profile is given by (24). Then one obtains that

$$\nabla \approx \frac{1}{4} \left(2 \frac{R_L^2}{R_B r} + 3 \frac{R_L^2}{R_B \lambda} \right) \ll 1, \quad (39)$$

i.e. atmosphere is convectively stable above the photosphere. Below the photosphere, for $r \lesssim R_{ph}$, temperature is related to pressure by (35) which results in

$$\begin{aligned} \nabla(T) &= \nabla_0 \left\{ 1 - \left(\frac{T_{ph}}{T} \right)^{4-\beta} \right. \\ &\times \left. \left[1 - \frac{3}{4\nabla_0} \frac{R_L^2}{R_B \lambda} \left(\frac{P_{ph}}{P_0} \right)^{1+\alpha} \left(\frac{T_0}{T_{ph}} \right)^{4-\beta} \right] \right\}. \end{aligned} \quad (40)$$

Since according to (33) & (34) $T_{ph} \approx T_0$ and $(P_{ph}/P_0)^{1+\alpha} \approx \lambda/R_B$, one finds that ∇ below R_{ph} is still given by (38) with the relative accuracy $O(R_L^2/R_B^2) \ll 1$. Consequently, in the optically thin case (22) atmosphere is convectively stable everywhere above R_a , analogous to the optically thick case. Thus, in both cases considered in §3.3.1 and 3.3.2 there is an *outer radiative (convectively stable) region* in the atmosphere, which is almost isothermal.

Deep in the envelope, below R_a , radiative temperature gradient is given by (38) and steadily increases with depth (since T monotonically goes up); deep inside the envelope ∇ becomes equal to ∇_0 . Thus, whenever

$$\nabla_0 = \frac{1+\alpha}{4-\beta} < \nabla_{ad} = \frac{\gamma-1}{\gamma} \quad (41)$$

the whole envelope is convectively stable and energy is transferred from the bottom by radiative diffusion. If opacity is independent of P and T , i.e. $\alpha = \beta = 0$, then $\nabla_0 = 1/4$ (Stevenson 1982) and envelope is convectively

stable provided that it is composed of monoatomic or diatomic gas.

In the opposite case, when $\nabla_0 > \nabla_{ad}$ envelope becomes convectively unstable at some point. From (38) we find that this happens when gas temperature reaches

$$T_{conv} \approx T_0 \left(1 - \frac{\nabla_{ad}}{\nabla_0} \right)^{-1/(4-\beta)} \quad (42)$$

This critical temperature above which convection sets in is clearly not very different from T_0 . Thus, T_{conv} is achieved at $\approx R_a$ from the core center and we conclude that atmosphere becomes convective below $\approx R_a$. For example, when the dominant source of opacity in the outer atmosphere is dust with $\beta = 1$, one should expect envelope to be convectively unstable if H_2 is its major constituent. In this case convection sets in at $T_{conv} = 7^{1/3} T_0 \approx 1.9 T_0$. The edge of the convection zone as shown in Figures 3 and 4 agrees with this estimate.

If envelope is convectively unstable below R_a , equation (7) cannot be used there. Instead, one has to utilize (8) to relate pressure and density in (5). Value of K in (8) is set by the conditions at the edge of the convection zone, i.e. at $T = T_{conv}$. In the optically thin atmospheres (see §3.3.2) pressure at this point is set by (35) to be

$$\begin{aligned} P_{conv} &\equiv P_0 \left\{ \left(\frac{P_{ph}}{P_0} \right)^{1+\alpha} \right. \\ &+ \left. \frac{4\nabla_0}{3} \frac{R_B \lambda}{R_L^2} \left[\frac{1}{1 - \nabla_{ad}/\nabla_0} - \left(\frac{T_{ph}}{T_0} \right)^{4-\beta} \right] \right\}^{1/(1+\alpha)} \\ &\approx P_0 \left[\frac{4}{3} \frac{\nabla_{ad} \nabla_0}{\nabla_0 - \nabla_{ad}} \frac{R_B \lambda}{R_L^2} \right]^{1/(1+\alpha)}. \end{aligned} \quad (43)$$

The last line in (43) follows from (34) and $T_{ph} \approx T_0$. Apparently, $P_{conv} \sim P_a \gg P_0$. In the optically thick atmospheres pressure is given by (23), which can be obtained from (35) by setting $P_{ph} = P_0$ and $T_{ph} = T_0$. Making the same substitutions in equation (43) we find that P_{conv} is still given by (43), despite the different structure of the outer radiative layer.

Solving equations (5) and (8) with the boundary condition $\rho = \rho_{conv} \equiv P_{conv} \mu / k T_{conv}$ at $r \approx R_a$ and using $K = P_{conv} \rho_{conv}^{-\gamma}$ one finds

$$\begin{aligned} \rho(r) &= \rho_{conv} \left[1 + \nabla_{ad} \frac{GM_c}{K \rho_{conv}^{\gamma-1}} \left(\frac{1}{r} - \frac{1}{R_a} \right) \right]^{1/(\gamma-1)} \\ &= \rho_{conv} \left[1 + \nabla_{ad} \left(1 - \frac{\nabla_{ad}}{\nabla_0} \right)^{1/(4-\beta)} \left(\frac{R_B}{r} - \frac{R_B}{R_a} \right) \right]^{1/(\gamma-1)} \end{aligned} \quad (44)$$

For $r \lesssim R_a(1 - R_a/R_B)$ gas density strongly exceeds ρ_{conv} and one obtains

$$\left(\frac{\rho}{\rho_{conv}} \right)^{\gamma-1} = \frac{T}{T_{conv}} \approx \nabla_{ad} \frac{T_0}{T_{conv}} \left(\frac{R_B}{r} - \frac{R_B}{R_a} \right) \quad (45)$$

Note that this temperature profile would be identical to (28) found for envelopes with radiative interiors if ∇_{ad} were replaced with ∇_0 ; apparently, temperature behavior is not very sensitive to the details of physics determining the atmospheric structure.

4. ATMOSPHERES WITH OUTER CONVECTIVE ZONE.

Whenever planetesimal accretion luminosity is high, luminosity radius R_L can exceed R_B in the optically thin case (c.f. §3.3.2) or $(R_B\lambda)^{1/2}$ in the optically thick (c.f. §3.3.1). Based on the results of §3 we can anticipate that intense energy release at the core surface would strongly affect gas temperature even beyond the Bondi radius, and this qualitatively changes the atmospheric structure.

We will concentrate on the optically thick case with

$$R_B \gg \lambda, \quad R_L^2 \gtrsim R_B\lambda \quad (46)$$

(directly opposite to [21]), typical in the terrestrial region (see Figure 2). Since atmosphere is optically thick equation (23) should determine the envelope structure if it were convectively stable. However, it is easy to show that under the conditions (46) gas around the core cannot be convectively stable even at $R_{out} \gg R_B$! Indeed, temperature gradient is given by (37) and one finds that far from the core $\nabla > \nabla_{ad}$ provided that

$$\nabla_{ad} < \nabla(\infty) = \frac{3}{4} \frac{R_L^2}{R_B\lambda} = \frac{3}{64\pi} \frac{L\kappa_0\rho_0c_0^2}{GM_c\sigma T_0^4}. \quad (47)$$

If (46) holds, $\nabla \approx R_L^2/(R_B\lambda) \gg 1$ already at $r \sim R_{out}$, meaning that even the outer part of the envelope is convective. This is completely different from the situation typical for the region of giant planets (see §3) where conditions are such that protoplanetary envelopes always have an almost isothermal outer radiative zone. The reason for this difference is that in the present case large energy flux escaping from the core severely affects gas temperature outside Bondi sphere where gas pressure is still almost equal to its nebular value P_0 . Consequently, temperature gradient $\partial \ln T / \partial \ln P$ takes on a high value outside of R_B (unlike the case studied in §3) giving rise to convection. As a result, envelope acquires an *outer convective zone*.

Calculation similar to that leading to (44) yields the following density structure in the convective part of atmosphere:

$$\rho(r) = \rho_0 \left[1 + \nabla_{ad} \left(\frac{R_B}{r} - \frac{R_B}{R_{out}} \right) \right]^{1/(\gamma-1)}. \quad (48)$$

This expression shows that gas density, pressure, and temperature deviate weakly from their nebular values ρ_0 , P_0 , and T_0 as long as $R_B \lesssim r \lesssim R_{out}$, but they increase as power laws of R_B/r inside the Bondi sphere. Apparently, internal atmospheric structure (for $r \lesssim R_B$) is rather insensitive to a particular choice of radius R_{out} at which boundary conditions (20) are set, as long as $R_{out} \gtrsim R_B$.

Structure of the interior regions of the envelope depends on the opacity behavior as described in §3.3.3: atmosphere is convective from R_{out} all the way to R_c whenever $\nabla_0 > \nabla_{ad}$, but it becomes convectively stable and radiative at some depth if $\nabla_0 < \nabla_{ad}$. In the latter case, for the inner radiative region to exist it is necessary that convection stops above the core surface. Suppose that $\nabla_0 < \nabla_{ad}$ and that transition between the outer convective zone and the inner radiative region takes place at a distance R_{rad} from the core center. Pressure, temperature, and density at this point are P_{rad} , T_{rad} , ρ_{rad} ; they can be uniquely related to R_{rad} by (48) since the outer boundary of the radiative zone is also an inner boundary

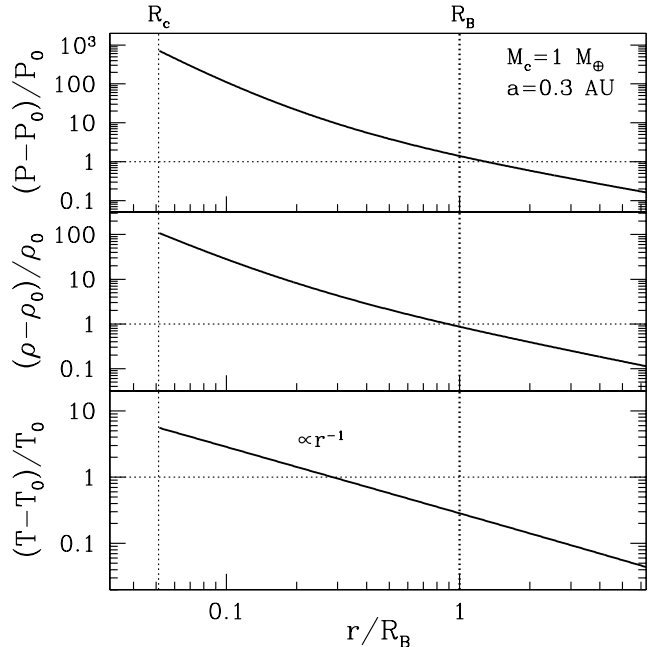


FIG. 5.— Same as Figure 3 but for $M_c = 1 M_\oplus$ at 0.3 AU. In this particular case $P_0 = 3 \times 10^{-3}$ bar, $\rho_0 = 1.6 \times 10^{-7}$ g cm $^{-3}$ and $T_0 = 550$ K. Also $\lambda \ll R_B$ and $R_B\lambda/R_L^2 \approx 0.06$, i.e. envelope is optically thick everywhere and possesses an outer convective zone, see §4. The interior of this atmosphere is also convective for a particular choice of parameters (the same as for Figure 3) used in producing this Figure.

of the convective zone. Within the radiative zone behavior of $\nabla(T)$ can be described by (40) with P_{ph} and T_{ph} replaced by P_{rad} and T_{rad} . Then one can easily fix the value of R_{rad} from the condition $\nabla(T_{rad}) = \nabla_{ad}$:

$$R_{rad} \approx R_B \frac{\nabla_{ad}}{\Theta}, \quad \Theta \equiv \left(\frac{3}{4\nabla_{ad}} \frac{R_L^2}{R_B\lambda} \right)^{\frac{\nabla_{ad}}{(4-\beta)(\nabla_{ad}-\nabla_0)}} \quad (49)$$

It is clear that $\Theta \gg 1$ and $R_{rad} \ll R_B$ because of (46). Inner radiative zone exists only if $R_{rad} > R_c$ in addition to $\nabla_0 < \nabla_{ad}$. Temperature and density at R_{rad} are, of course, much larger than T_0 and P_0 : $T_{rad}/T_0 = (\rho_{rad}/\rho_0)^{\gamma-1} \approx \Theta$, see (48).

We also briefly discuss the atmospheric structure in the optically thin case³

$$R_B \ll \lambda, \quad R_B \ll R_L \quad (50)$$

opposite to that considered in §3.3.2. Using equation (31) to determine the temperature structure in the optically thin part of the envelope one finds T to be strongly perturbed beyond the Bondi radius because of the second inequality in (50). Then it is rather clear that such atmospheres should possess outer convective zones, similar to the case when (46) holds. This conclusion is independent upon the relationship between R_L and λ . We do not consider the interior structure of such envelopes in this study.

³ This particular relationship between R_B , R_L , and λ can be realized only in the region of giant planets for small cores accreting in the fast regime, see Figure 2. We mention it here mainly for completeness.

5. ENVELOPE MASS AND CRITICAL CORE MASS.

We define mass of the envelope M_{env} as

$$M_{env} \equiv 4\pi \int_{R_c}^{R_B} \rho(r') r'^2 dr', \quad (51)$$

where we have chosen R_B to be the outer boundary of the envelope. We compute M_{env} separately for atmospheres with the outer radiative and convective zones since it will turn out that masses are very different in the two cases. Using these results we also estimate the critical core mass necessary for the initiation of a runaway gas accretion in §5.5.3.

5.1. Envelopes having outer radiative zone.

Results of §3 demonstrate that gas density in the atmospheres having outer radiative zone increases exponentially between R_B and R_a . As a result, most of the atmospheric mass is contained within $\sim R_a$. In Appendix B we demonstrate that M_{env} is given by

$$M_{env} \approx 4\pi \Psi_1 \rho_0 R_B^3 \left(\frac{R_B \lambda}{R_L^2} \right)^{1/(1+\alpha)}, \quad (52)$$

where Ψ_1 is a weak (logarithmic) function of $R_B \lambda / R_L^2$ given by (B1). Envelope mass is dominated by the contribution coming from $r \sim R_a$ in all dynamically stable atmospheres with convective interiors and in all atmospheres with radiative interiors having $\nabla_0 > 1/4$; in these cases the inner part of the atmosphere near the core contributes to M_{env} only weakly, see Appendix B. We restrict ourselves to studying only these two important classes of envelopes.

Of special interest is the case when atmospheric opacity is independent of pressure (and, consequently, density), i.e. $\alpha = 0$. Then, regardless of whether envelope interior is radiative or convective, one finds using (12), (14), (15), (26), and (A1) that

$$M_{env} = 64\pi^2 \Psi_1 \left(\frac{GM_c \mu}{k} \right)^4 \frac{\sigma}{\kappa_0 L} \\ \approx \left(\frac{M_c}{M_\oplus} \right)^{8/3} \frac{0.1 \text{ cm}^2 \text{ g}^{-1}}{\kappa_0} \begin{cases} 8 \times 10^{27} \text{ g } a_{10}^3, & \text{slow,} \\ 6 \times 10^{24} \text{ g } a_{10}^2, & \text{int.} \\ 2 \times 10^{23} \text{ g } a_{10}^{3/2}, & \text{fast.} \end{cases} \quad (53)$$

Different numerical estimates are for three accretion regimes described in Appendix A and assume molecular gas of cosmic composition, $\beta = 1$, and $\gamma = 7/5$ (convective interior). The peculiarity of this special case is that envelope mass is virtually independent of the temperature and density in the surrounding nebula. Indeed, both T_0 and ρ_0 enter (53) only logarithmically through the dependence of Ψ_1 on R_B/R_a , see (26) and (B1). Local conditions in the protoplanetary disk affect M_{env} only through gas opacity κ_0 and planetesimal accretion luminosity L . This was first noticed by Stevenson (1982) who discovered this feature while studying radiative envelopes with constant gas opacity, $\alpha = \beta = 0$. But equation (53) demonstrates that insensitivity of M_{env} to T_0 and ρ_0 is a more general phenomenon since it holds even when atmospheric opacity varies with temperature and for convective as well as radiative interiors, provided only that $\alpha = 0$, i.e. opacity is independent of the gas density.

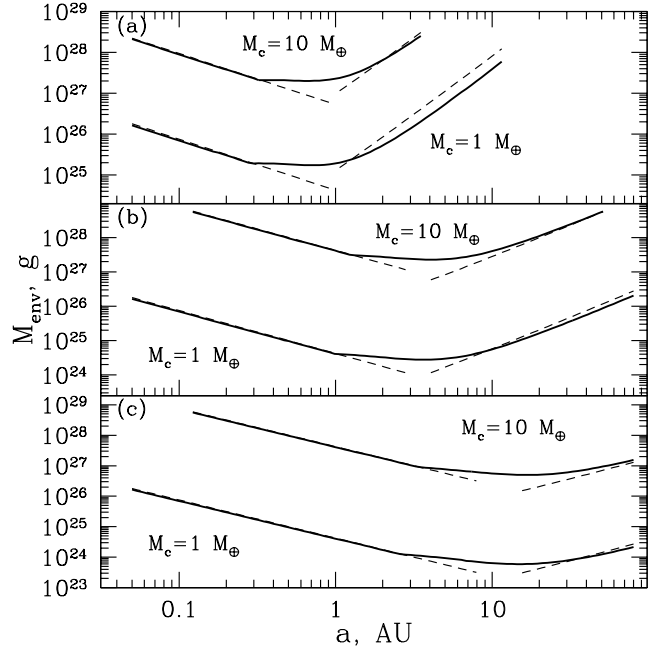


FIG. 6.— Mass of the envelope for two values of $M_{core} = 1, 10 M_\oplus$ as a function of semi-major axis a in the nebula. Different panels correspond to different planetesimal accretion regimes: (a) slow, (b) intermediate, and (c) fast. Solid curves labeled with corresponding core masses represent results of numerical calculation of M_{env} . Dashed lines display analytical estimates of M_{env} for the same M_c given by (53) and (55) for large and small a respectively.

When κ does depend on pressure ($\alpha \neq 0$), one finds that

$$M_{env} \propto \left[\frac{\rho_0^\alpha (M_c \mu)^{4+3\alpha}}{T_0^{3\alpha} \kappa_0 L} \right]^{1/(1+\alpha)}, \quad (54)$$

i.e. envelope mass depends on nebular properties in this more general case. But even then the detailed character of dependence is not determined by whether atmospheric interior is radiative or convective, but only by the opacity dependence on P .

It might seem surprising that mass of the envelope with convective interior can be sensitive to the gas opacity since the energy transfer below R_a is not done by radiation. The explanation lies in the presence of the outer radiative zone above R_a which is non-adiabatic. Because of that gas entropy at the edge of the convective zone (at $\approx R_a$) is set by the radiative energy transfer in the outer atmosphere and depends on the gas opacity κ_0 (see equation [59]). This is the origin of dependence of M_{env} on the nebular opacity in the case of atmospheres with convective interiors.

In Figure 6 we plot M_{env} for cores of specified mass (1 and $10 M_\oplus$) as a function of core's distance from the Sun a for fast, intermediate, and slow planetesimal accretion regimes (see Appendix A). Numerical results of the envelope structure calculations for $\alpha = 0, \beta = 1, \kappa_0 = 0.1 \text{ cm}^2 \text{ g}^{-1}, \gamma = 7/5$ are shown by solid curves; dashed line at large a is our analytical estimate of M_{env} given by (53). As Figure 6a demonstrates, formula (53) somewhat overestimates M_{env} : because of the finite size of the core our extension of integration in (B1) to zero (instead of R_c) leads to the overestimate of M_{env} ; relative

correction is $\sim (R_c/R_a)^{1/2}$ which is small but sometimes non-negligible. We checked that this discrepancy goes away when we artificially set R_c to 0 in our numerical calculations.

5.2. Envelopes having outer convective zone.

Mass of the atmosphere possessing outer convective zone is calculated using density profile (48). Assuming that (48) holds up to the core's surface (fully convective envelope, $\nabla_0 > \nabla_{ad}$) one finds

$$M_{env} = 4\pi\Psi_2\rho_0R_B^3 \approx 4 \times 10^{24} \text{ g} \left(\frac{M_c}{M_\oplus}\right)^3 a_1^{-5/4},$$

$$\Psi_2(\gamma) \equiv \int_0^1 z^2 \left(1 + \frac{\nabla_{ad}(\gamma)}{z}\right)^{1/(\gamma-1)} dz, \quad (55)$$

where we have assumed $R_B/R_{out} \lesssim 1$. Numerical estimate is done for $\gamma = 7/5$ ($\Psi_2 \approx 0.88$). Similar estimate of M_{env} can be found in Wuchterl (1993).

A remarkable property of atmospheres having outer convective zone is that gaseous mass contained within a Bondi sphere around the core is of the order of the mass of nebular gas with $\rho = \rho_0$ contained within the same volume! This is very different from atmospheres possessing outer radiative region, which not only have envelope mass much higher than $(4/3)\pi\rho_0R_B^3$, but also contain this mass within smaller volume than that of the Bondi sphere, see (52). In addition, M_{env} given by (55) is completely independent of the core luminosity and gas opacity, very much unlike the case studied in §5.1.

Most of the mass in fully convective atmospheres is concentrated in their outer part (because of the requirement $\gamma > 4/3$ necessary for dynamical stability), which allowed us to set the lower integration limit in the definition of Ψ_2 to zero. One can demonstrate that in the case of envelopes having inner radiative region (those with $\nabla_0 > \nabla_{ad}$) formula (55) continues to correctly describe the mass of the envelope, provided that $\nabla_0 \geq 1/4$ in its radiative part (because most of the mass in radiative region is then concentrated near its outer edge); also, inner radiative region typically has rather small radial extent, see (26).

In Figure 6 analytical estimate (55) is displayed by the dashed line in the inner part of the nebula (terrestrial planet region, $\lesssim 1$ AU). One can see very good agreement of analytical result with the predictions of more detailed numerical calculations.

5.3. Critical core mass.

As we have mentioned in the Introduction, both numerical calculations and analytical arguments suggest that phase of rapid gas accretion onto the protoplanetary core initiates when $M_{env} \sim M_c$. The exact ratio of the two masses at the onset of instability is uncertain and can be determined only after the envelope's self-gravity is self-consistently taken into account which is beyond the scope of this study. Here we simply assume this critical ratio to be a free parameter $\eta \sim 1$, so that

$$M_{env}(M_{cr}) = \eta M_{cr}, \quad (56)$$

where M_{cr} is the critical core mass at the onset of rapid gas accretion. For a fixed η instability condition (56) can be viewed as an equation for M_{cr} .

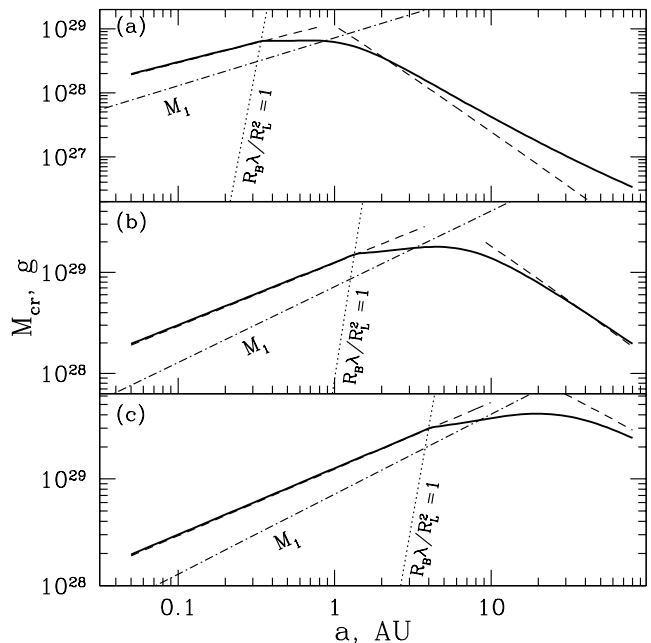


FIG. 7.— Critical core mass as a function of semi-major axis a in the nebula for (a) slow, (b) intermediate, and (c) fast planetesimal accretion rates. Solid curve represents numerical results, while dashed lines display estimates of M_{cr} given by (57) and (58) at large and small a correspondingly. Dot-dashed line shows the run of fiducial mass M_1 (equation [16]) with a .

Using (9), (53), and (A1) we find that for atmospheres having outer radiative region (§3) critical core mass is given by

$$M_{cr} = \left[\frac{\eta\theta}{64\pi^2\Psi_1} \frac{\Omega\Sigma_p a\kappa}{\sigma G^3 M_\odot^{1/3}} \left(\frac{k_0}{\mu}\right)^4 \right]^{3/5}$$

$$\approx \eta_{0.3}^{3/5} \left(\frac{\kappa_0}{0.1 \text{ cm}^2 \text{ g}^{-1}}\right)^{3/5} \begin{cases} 2.4 \times 10^{27} \text{ g } a_{10}^{-9/5}, & \text{slow,} \\ 1.9 \times 10^{29} \text{ g } a_{10}^{-6/5}, & \text{intermediate,} \\ 1.5 \times 10^{30} \text{ g } a_{10}^{-9/10}, & \text{fast,} \end{cases} \quad (57)$$

where $\eta_{0.3} \equiv \eta/0.3$ and θ is a parameter determining the efficiency of accretion. Apparently, core instability sets in at lower M_c in the more distant parts of the nebula because of the rapid decrease of planetesimal accretion rate \dot{M} with a . Note a strong dependence of M_{cr} on the mean molecular weight μ (Stevenson 1982). Convective erosion of the core and dissolution of infalling planetesimals in the envelope might increase μ and considerably lower M_{cr} , facilitating rapid gas accretion.

Opacity determining M_{env} and M_{crit} in (52) and (57) is the opacity *in the outer radiative zone only* — it is the radiation transfer in this region that determines the conditions in the innermost part of the envelope and, hence, its mass. Temperature in the radiative zone does not deviate strongly from T_0 and we can be more confident that the opacity behavior in this region can be represented by a simple power law dependence (13). This assertion becomes even more robust if opacity there is also independent of gas density (since density strongly varies within the radiative zone), and this is the case when opacity is dominated by dust absorption.

In the case of atmosphere having outer convective zone

(§4) we find after substituting (55) into (56) that

$$M_{cr} = c_0^3 \left(\frac{\eta}{4\pi\Psi_2\rho_0 G^3} \right)^{1/2} \approx 1.2 \times 10^{29} \text{ g } \eta_{0.3}^{1/2} a_1^{5/8} \quad (58)$$

This critical mass decreases as one goes *inward* in the nebula (unlike [57]) because gas density in the disk rapidly increases inward. Introducing the Toomre stability parameter $Q \equiv \Omega c_0 / (\pi G \Sigma_g)$ one can rewrite (58) as $M_{cr} = (Q/4\Psi_2)^{1/2} M_1$, see definition (16). This implies that $M_{cr} \gtrsim M_1$ in gravitationally stable protoplanetary disks⁴ with $Q \gtrsim 1$. It is then clear that M_{env} given by (58) is only a rough estimate of the critical core mass because nebula cannot be considered static and homogeneous on the scale of R_B (as we always assumed) when $M_c > M_1$, see §2.2.2.

Comparing (52) with (55) we see that presence of the outer radiative zone, requiring $R_B \lambda \gg R_L^2$, increases M_{env} and lowers M_{cr} . This happens because radiative diffusion across almost isothermal outer radiative zone significantly reduces the entropy of the inner envelope. Lower entropy means higher density resulting in a higher M_{env} compared to the mass which an isentropic atmosphere would have for the same core mass. For instance, in the optically thick atmosphere with $R_B \lambda \gg R_L^2$ the value of adiabatic constant K at R_a is

$$K \sim K_0 \left(\frac{R_L^2}{R_B \lambda} \right)^{(\gamma-1)/(1+\alpha)}, \quad (59)$$

see [42], [43], and [44]; $K_0 \equiv P_0 \rho_0^{-\gamma}$ is the adiabatic constant of gas in the surrounding nebula. It follows from (59) that $K \ll K_0$, i.e. gas entropy in the inner atmosphere is *much lower* than it is in the surrounding nebula. Consequently, M_{cr} for an atmosphere with the outer radiative zone is lower than it would have been if atmosphere were isentropic (i.e. had outer convective zone).

In Figure 7 we plot the critical core mass as a function of a for different planetesimal accretion regimes, self-consistently taking into account transition between different types of atmospheres in the inner and outer parts of protoplanetary disk. In addition to the results of numerical calculations of the atmospheric structure we also plot analytical approximations for M_{cr} given by (58) in the region of terrestrial planets and by (57) in the region of giant planets. In the terrestrial planet region theory and numerical calculations agree very well and one can see that $M_c > M_1$ in agreement with what we have said before ($Q \gtrsim 30$ at $a \lesssim 1$ AU for the MMSN parameters given by [2]). In the giant planet region there are discrepancies between the theory and numerical results at large a which are especially pronounced in Figure 7a. They appear because of the finite size of the core which causes (53) to overestimate M_{env} , see §5.1; in the more careful numerical calculation a bigger core is required to trigger the runaway gas accretion.

6. DISCUSSION.

One of the major results of our study is a clear distinction between protoplanetary atmospheres having convective outer region which smoothly merges with the surrounding nebula and atmospheres having radiative zone

separating dense and hot interior from the nebula. A specific type of atmosphere around a particular protoplanetary core is determined by the relationships between three important length scales — R_B , R_L , and λ — provided that core mass satisfies the mass constraint (19). Whenever planetesimal accretion rate of the core is low, meaning that R_L is small (i.e. either [21] or [22] is fulfilled), gas temperature can be appreciably affected only deep inside the Bondi sphere while the pressure starts to vary already at the Bondi radius. As a result, according to the Schwarzschild criterion (6), outer parts of the envelope are convectively stable and energy is carried away by radiation. In the opposite case of very high accretion rate and large R_L (i.e. either [46] or [50] holds), gas temperature is perturbed even outside the Bondi sphere, and condition (6) predicts that gas is convectively unstable for $r \gtrsim R_B$, where pressure perturbation is small. Moreover, in the latter case even if the innermost parts of the envelope tend to settle onto the radiative (convectively stable) configuration, they would be able to switch to a radiative solution only very deep in the envelope, see equation (49).

This segregation of atmospheres into two major classes depends to some extent on whether the outer parts of the atmosphere are optically thick or thin. For example, envelope structure in the optically thick case depends only on the value of the dimensionless parameter $\lambda R_B / R_L^2$ — roughly the inverse of the radiative temperature gradient far from the core (see [12], [14], [15], and [D1]), and is completely insensitive to the individual relationships between λ , R_L , and R_B (as long as $\lambda \ll R_B$): envelope has outer convective zone when $\lambda R_B / R_L^2 \lesssim 1$ and outer radiative zone when $\lambda R_B / R_L^2 \gtrsim 1$. Analogous condition was formulated by Wuchterl (1993) in terms of nebular density ρ_0 . Separation between the two classes of atmospheres in the optically thin case is somewhat more complicated (e.g. see constraint [22]) and one has to pay attention to the individual relationships between the three length scales. Results of §3 & 4 cover all such possibilities.

Because these characteristic length scales vary with the distance from the Sun, a specific type of atmosphere forming around the core of a given mass depends on a . This is caused primarily by the variation of the planetesimal accretion rate throughout the protoplanetary disk: in the terrestrial region the planetesimal surface density is high while the dynamical timescale is short leading to high \dot{M} , large R_L , and small $R_B \lambda / R_L^2$. Another important factor is a steep dependence of λ on a (see Figure 1). As a result, atmospheres around massive cores in the inner parts of protoplanetary disks (within roughly 0.5 – 2 AU depending on the planetesimal accretion regime) where $R_B \lambda \lesssim R_L^2$ possess outer convective zones, see Figure 2a. On the contrary, in the region of giant planets both Σ_p and Ω are small, which decreases \dot{M} making R_L small as well. Photon mean free path there is large because gas density is very low (disk can be optically thin). These factors conspire to rapidly increase $R_B \lambda / R_L^2$ with a and allow cores outside of $\sim (0.5-2)$ AU to have massive atmospheres with quite extended outer radiative zones, see Figures 3 & 4. Some exceptions are possible (e.g. cores having $R_B \ll \lambda$ and $R_B \ll R_L$ in the region of giant planets have convective outer atmo-

⁴ Similar argument was advanced in Ikoma et al. (2001).

spheres, see §4 and Figure 2) but they typically occur for rather small cores unable of retaining massive atmospheres.

6.1. Comparison with previous studies.

Envelopes with the outer convective region have been previously considered by Perri & Cameron (1974), Wuchterl (1993), and Ikoma et al. (2001), who found the masses of such envelopes to be rather small which translated into large critical core mass. In addition, properties of such fully convective atmospheres were found to strongly depend on the temperature and density in the surrounding nebula. This is exactly the picture that we described in §4. Wuchterl (1993) suggested that the sensitivity to external conditions is a consequence of envelopes being fully convective, but as we demonstrate in §4 what is really important is the convection *in the outermost region of atmosphere* only, independent of whether the atmospheric interior is convective or radiative. Presence of the outer convective region sets entropy of the inner atmosphere equal to the entropy of the nebular gas, so that variations in the external conditions directly affect the overall structure (and mass) of the envelope. Nebular entropy is quite high, which makes atmospheres not very dense and accounts for the low masses of such envelopes, see Figure 6. As our analysis demonstrates, Perri & Cameron (1974) and Wuchterl (1993) have probably stretched their assumptions too far by calculating $M_{cr} \approx 60 M_{\oplus}$ for convective envelopes at 5 AU, in the region of giant planets, where atmospheres should in fact have outer radiative (not convective) zones.

Envelopes possessing a radiative region between the inner, dense parts of the atmosphere and the nebular gas outside have first been studied numerically by Harris (1978), Mizuno et al. (1978), and Hayashi et al. (1979). Mizuno (1980) and Stevenson (1982) were the first to notice that presence of the outer radiative region makes critical core mass virtually independent upon the density and temperature of the surrounding gas, provided that the opacity in the outer atmosphere is *constant*, i.e. κ is independent of either gas pressure or temperature ($\alpha = \beta = 0$). This is completely different from envelopes having outer convective region and occurs because outer radiative zone decouples inner atmosphere from the surrounding nebula. As we demonstrated in §5.1 this insensitivity of M_{cr} to the external nebular conditions holds also in a more general case of $\alpha = 0$ and arbitrary β (opacity independent on the gas density), see equation (53). This scaling is typical for the dust opacity which should dominate⁵ over the molecular opacity due to H₂ and H₂O under the conditions typical in the outer radiative zone, see opacity plots in Hayashi et al. (1979) and Mizuno (1980) and Figures 3 & 4. Thus, one would naturally expect envelope mass and critical core mass to be independent of ρ_0 and T_0 (except for the local value of opacity κ_0 which may scale with local temperature T_0); this result is also completely insensitive to the structure of the innermost part ($r \lesssim R_a$) of the envelope, be it radiative or convective. Of course, as soon as α is nonzero, this degeneracy breaks and critical core mass starts to depend on T_0 and ρ_0 , as equation (54) demonstrates.

Previous studies self-consistently accounting for the

presence of the outer radiative zone (Hayashi et al. 1979; Mizuno 1980; Stevenson 1982; Nakazawa et al. 1985; Ikoma et al. 2000) have found $M_{cr} \sim 10 M_{\oplus}$, depending on the dust opacity and accretion luminosity of the core. These authors typically assumed constant \dot{M} , i.e. $M_c \propto \tau$, while we consider several possible accretion regimes taking into account the dependence of \dot{M} on the core mass and its distance from the Sun. Note that for the same core formation timescale our assumed accretion law $M_c \propto \tau^3$ (see Appendix A) yields higher \dot{M} in the end of core accretion than constant \dot{M} does; this acts to increase M_{cr} . If nucleated instability sets in when envelope mass is 30% of the core mass and $\kappa_0 = 0.1 \text{ cm}^2 \text{ g}^{-1}$, as we assumed in all our numerical estimates, we find that critical core mass in the fast regime of planetesimal accretion is $53 M_{\oplus}$ at 5 AU (present Jupiter’s location) and $62 M_{\oplus}$ at 10 AU (current Saturn’s location). In the intermediate accretion regime M_{cr} is $30 M_{\oplus}$ and $23 M_{\oplus}$ at 5 and 10 AU correspondingly; it drops to $1.8 M_{\oplus}$ and $0.7 M_{\oplus}$ at these locations in the slow accretion regime. Ikoma et al. (2000) have found values of M_{cr} that are somewhat lower (sometimes by ~ 2) than those found in this work for the same \dot{M} and κ_0 because they used opacity in the outer atmosphere independent of P and T which has effect of increasing M_{env} (see below) while we use realistic dust opacity. Our neglect of atmospheric self-gravity is another reason for this difference.

Inner envelope ($r \lesssim R_a$) can be either radiative or convective, depending on the detailed opacity behavior. We found that this part of atmosphere is radiative provided that α and β in (13) are such that the condition (41) is fulfilled; if $\nabla_0 > \nabla_{ad}$ the inner envelope must be convective. Stevenson (1982) used constant opacity in his study which made the entire envelope convectively stable and energy was transferred solely by radiation. On the other hand, in the important case of opacity dominated by small dust grains one would take $\alpha = 0$ and $\beta \approx 1 - 2$. Equation (41) demonstrates that envelopes with such opacity should be convectively unstable if they consist of diatomic gas with $\gamma = 7/5$, see Figures 3 & 4.

Of course, dust opacity cannot dominate in the whole envelope — at large depth pressure and temperature are so high that H₂ and H₂O opacities become more important, and their behavior cannot be described by a simple power law dependence (13). Hayashi et al. (1979) and Mizuno (1980) showed that envelope is typically *convectively unstable* when these molecular opacities dominate. In addition to molecular κ these authors also included constant dust opacity similar to Stevenson (1982), which had the effect of making atmosphere radiative in the outer region where κ was dominated by dust and convective at greater depth where molecular opacity was more important. In their case this transition typically occurred quite deep in the envelope, way below what we would call R_a . Presence of such extensive radiative zone increases M_{env} and decreases M_{cr} : as long as $\alpha = \beta = 0$, density in the radiative region varies as r^{-3} and atmospheric mass is evenly distributed in equal logarithmic intervals in r , see Appendix B. This augments total envelope mass compared to the mass contained in just the outermost part near R_a by additional factor equal to the logarithm of ratio of the outer to inner radii of this radiative zone (and this ratio is large). But if one

⁵ Unless the dust opacity is very small, $\lesssim 10^{-2} \text{ cm}^2 \text{ g}^{-1}$

uses opacity with $\nabla_0 > \nabla_{ad}$ then there is no radiative region below R_a , envelope becomes convective at much smaller depth, right below R_a , and most of the atmospheric mass is concentrated near R_a , see Appendix B. We expect the latter to occur [and M_{cr} to be higher than what Hayashi et al. (1979), Mizuno (1980) and Ikoma et al. (2000) have found] whenever opacity is dominated by small dust grains, since $\alpha = 0$ and $\beta \approx 1 - 2$ in this case. Convection at small depth in the case of dust opacity also wipes out the need to know the molecular opacities deep inside the atmosphere very accurately: behavior of κ there is irrelevant as long as envelope is convective below R_a .

6.2. Critical mass: implications for planet formation.

Our results for the critical core mass necessary to trigger the nucleated instability fall within the range of previously estimated values of M_{cr} . In the terrestrial planet region, at 1 AU, we estimate⁶ $M_{cr} \approx 20 M_{\oplus}$ if planetesimal accretion is in the intermediate or fast regime: $R_B \lambda / R_L^2 \lesssim 1$ in both cases, meaning atmosphere with outer convective zone. Perri & Cameron (1974) and Wuchterl (1993), who studied convective envelopes, would have obtained the same value of M_{cr} if they were to calculate it at 1 AU.

At the same time, accretion in the intermediate or fast regime which keeps R_L high can only proceed for rather limited time span at ~ 1 AU until the isolation mass is reached (Lissauer 1993). Beyond this point protoplanetary cores accrete basically at their geometric cross-section, i.e. in the slow accretion regime (Appendix A; Goldreich et al. 2004), for which $R_B \lambda / R_L^2$ could be somewhat higher than 1. After this transition occurs, critical core mass at 1 AU goes down to about $10 M_{\oplus}$ (see Figure 7). Inward from 1 AU, in the region where “hot Jupiters” were discovered, M_{cr} decreases and reaches $\approx 5 M_{\oplus}$ at 0.1 AU. Since the amount of refractory material in the inner parts of protoplanetary disks is rather small and it takes very long time ($\sim 10^8$ yr, see Chambers 2001) to collect this material into $\sim 1 M_{\oplus}$ protoplanets, we conclude that cores forming in situ in the terrestrial zone would not be able to undergo nucleated instability before gas in the nebula has gone away (within $\sim 10^7$ yr). These considerations strengthen the argument according to which “hot Jupiters” or their massive progenitor cores have migrated to their present locations from elsewhere.

Although masses of existing terrestrial planets are clearly too low to drive the nucleated instability, they were high enough to retain quite substantial atmospheres while the nebular gas was still around. Our calculations demonstrate that $M_{env} = 4 \times 10^{21}$ g, 10^{25} g, 3×10^{25} g, and 3×10^{22} g for Mercury, Venus, Earth, and Mars correspondingly. This is to be compared with the present atmospheric masses of these planets: no atmosphere on Mercury, 5×10^{23} g, 5.2×10^{21} g, and 6.5×10^{18} g on Venus, Earth, and Mars. Clearly, the primaeval atmospheres of terrestrial planets have been heavily depleted. Massive primordial atmosphere can cause severe blanketing and melting of the core surface, effect which has been

first considered by Hayashi et al. (1979).

As we demonstrated in §6.1 critical core mass in the region of giant planets sensitively depends on the accretion regime: at 10 AU it is less than M_{\oplus} in the slow regime and as large as $60 M_{\oplus}$ in the fast. At the same time, present mass of the Jupiter’s solid core is estimated to be $\lesssim 10 M_{\oplus}$; current Saturn’s core mass is between $10 M_{\oplus}$ and $25 M_{\oplus}$ (Saumon & Guillot 2004). The initial core masses of these two planets could have been higher — their total masses in high-Z elements can be as high as $30 - 40 M_{\oplus}$ because some refractory materials can be dissolved in their envelopes. Transporting these elements from the core into the envelope would require some quite efficient mixing process such as vigorous convection (Stevenson 1982) and it is not clear at present if this is possible.

Accumulation of the solid cores in the giant planet region must have proceeded in the intermediate or fast accretion regime (or some combination of the two) because smaller \dot{M} would not allow solid cores to form before the nebula dissipation this far from the Sun. This translates into values of M_{cr} which are higher than the present core masses of Jupiter and Saturn. Thus, current data suggest that if cores were not initially more massive and subsequently eroded they were not large enough to trigger nucleated instability and accrete gas. The discrepancy is especially dramatic for Jupiter with its very low M_c . One way to resolve this paradox is to hypothesize that nebular opacity κ_0 was lower than $0.1 \text{ cm}^2 \text{ g}^{-1}$ which brings M_{cr} down, see (57). Another possibility is suggested by the observation that core formation in the intermediate or fast regime can take rather short time, of order several Myrs, see (A2). In this case, after the core of Jupiter has been mostly formed, there was still enough gas around to accumulate atmosphere. At this point, since the isolation mass has been reached, planetesimal accretion became considerably slower meaning that M_{cr} went down dramatically, below already accumulated M_c . As a result, gaseous envelope could not be supported by the energy release due to the significantly lowered \dot{M} and it started to slowly contract on a thermal timescale. Thus, the transition between different planetesimal accretion regimes must be accompanied by the period of envelope adjustment similar to that described in Introduction. After M_{env} reached $\sim M_c$ runaway gas accretion commenced. Similar scenario was studied numerically by Pollack et al. (1996) and Ikoma et al. (2000). We envisage the same picture to hold for Saturn as well, although its core must have taken longer to form than that of Jupiter and the nebula was appreciably depleted by that time; this may account for the smaller gaseous mass of Saturn.

Assembly of the cores of ice giants — Uranus and Neptune — would have required even more time. Relatively small atmospheres of these planets containing only $1 - 4 M_{\oplus}$ of H and He suggest that they either never underwent nucleated instability, or if they did this happened only after nebula has been very strongly depleted. In the former case all the gas that we see now in Uranus and Neptune has come from steady state atmospheres around the cores which were less massive than present cores of ice giants; after nebula went away these (sub-isolation mass) cores merged retaining their gaseous content (Genda &

⁶ Accurate value of M_{cr} in the terrestrial region can only be obtained after the effects of the vertical disk structure, differential shear, complicated flow geometry within the Hill sphere, etc. are properly included because in this part of protoplanetary disk $M_c > M_1$ (see §2.2.2 and Figure 7).

Abe 2003, 2004) and producing Uranus and Neptune. In the latter case fast accretion leads to the accumulation of isolation mass (essentially the present day mass of ice giants) and to subsequent nucleated instability before the nebula dispersal; however, if at that moment nebula was depleted by less than $10^2 - 10^3$, Neptune and Uranus would have much higher gaseous masses than they do now.

Critical mass rather strongly depends on the envelope composition, namely on μ . Stevenson (1982) was the first to notice this fact for purely radiative atmospheres. Our equation (57) confirms and generalizes this observation — we find $M_{cr} \propto \mu^{-12/5}$ for *any* envelope with the outer radiative zone (independent of whether its interior is radiative or convective). Dissolution of infalling planetesimals, erosion of the core by vigorous convection, or evaporation of some volatile icy content of the core can increase μ and decrease M_{cr} considerably (“super-ganymedeian puffballs”, Stevenson 1984). On the other hand, envelope enrichment in high-Z elements might also increase opacity in the outer atmosphere and this can at least partially counteract the decrease of M_{cr} due to large μ .

6.3. Validity of assumptions.

Because of the inherently analytical nature of this study aimed at singling out the most important aspects of atmospheric structure we have neglected a number of relevant phenomena which may be important in some cases. Among them are the dissolution of infalling planetesimals (Pollack et al. 1996), opacity jumps due to dust grain melting (Mizuno 1980), increase of planetesimal capture cross-section caused by the presence of the atmosphere (Inaba & Ikoma 2003), etc. We have also employed a set of simplifying assumptions such as hydrostatic and thermal equilibrium of atmosphere, negligible gas accretion luminosity, and so on. In Appendix C we demonstrate these assumptions to be valid. Our treatment of convection relies on the absence of entropy gradient in the convective regions and in Appendix D we checked whether this assumption is appropriate.

All our results are rather insensitive to the exact value of distance R_{out} at which atmosphere finally merges with the nebula as long as $R_{out} \gtrsim R_B$. This is because atmospheric pressure outside R_B is not very different from P_0 — planetary gravity cannot strongly perturb the pressure, while temperature is not very different from T_0 : in the case of envelopes having outer convective zone deviation of T from T_0 is directly related to the deviation of P from P_0 by the condition of adiabaticity and, consequently, must be small outside of Bondi sphere. In the case of envelopes having outer radiative zone temperature gradient is subadiabatic meaning that temperature deviation outside R_B is even smaller than in the convective case. As a result, atmospheric pressure and temperature are not very different from their nebular values already at R_B and the exact location where P and T closely match P_0 and T_0 is not very important.

Our use of opacity in the form (13) may seem an oversimplification compared to other treatments (e.g. Mizuno 1980; Ikoma et al. 2000) which employ realistic opacity tables. However, as mentioned previously, we expect κ in the outer part of the envelope to be dominated by dust and this typically (for $\beta \approx 1 - 2$) leads to

convection inward from R_a obviating the need to know the gaseous opacity behavior at high temperatures and pressures. Some effect on the envelope mass and critical core mass might come from the change of equation of state caused by dissociation and ionization in the deep interior of the atmosphere, which e.g. might lead to the appearance of radiative regions at large depth. However, since atmospheric mass budget is dominated by the outer part of the envelope at $r \sim R_a$, change of κ or γ deeper down hopefully would not strongly affect the value of M_{env} .

Thus, we expect our simple analytical treatment to provide robust qualitative picture of the envelope structure and its dependence upon local conditions in the protoplanetary disk, and yield reasonable quantitative estimates of M_{env} and M_{cr} .

7. CONCLUSIONS.

We investigated steady-state structure of the atmosphere around protoplanetary core immersed in the gaseous disk. Our major results can be summarized as follows.

Atmospheres split into those having outer convective or outer radiative (almost isothermal) zone. The former have entropy of the interior equal to the entropy of the surrounding nebular gas; the latter have interior entropy which is much lower than the nebular entropy, owing to the decoupling provided by the outer radiative region. Type of atmosphere around a given core is determined by the relationships between the Bondi radius R_B , photon mean free path λ , and luminosity radius R_L . If envelope is optically thick at the Bondi radius ($R_B \gg \lambda$) atmospheric type is set only by the value of the dimensionless parameter $R_B \lambda / R_L^2$, inverse of which has a meaning of radiative temperature gradient far from the core: outer envelope is convective when $R_B \lambda / R_L^2 \lesssim 1$, while when this parameter is $\gtrsim 1$ atmosphere has an outer radiative zone. For the conditions typical in the protoplanetary disks (such as MMSN) cores having atmospheres of the first kind are common in the terrestrial planet region; in the region of giant planets atmospheres have outer radiative zone. Structure of the atmospheric interior is determined by the dependence of opacity on gas temperature and pressure; it becomes especially simple (convective as soon as temperature starts to appreciably vary with depth) if opacity is dominated by small dust grains.

In the terrestrial region critical core mass for nucleated instability M_{cr} depends only on the local values of nebular gas density and temperature. In the region of giant planets M_{cr} is insensitive to either ρ_0 or T_0 whenever opacity in the outer radiative zone is independent of the gas pressure, because outer radiative zone decouples inner parts of the envelope from the nebular gas (irrespective of whether the atmospheric interior is radiative or convective); at the same time M_{cr} is a strong function of accretion luminosity, opacity, and mean molecular weight. Critical core mass varies as a function of distance from the Sun because of the variation of ρ_0 and T_0 in the terrestrial planet region and because of the variation of planetesimal accretion luminosity and photon mean free path in the region of giant planets. Typical value of M_{cr} is several tens of M_\oplus in the giant planet region (30 – 50 M_\oplus at 5 AU) if planetesimal accretion was fast enough to account for the core formation prior to the gas

dissipation. Close to the Sun, at $a \sim 0.1$ AU, $M_{cr} \approx 5 M_{\oplus}$ independent of the planetesimal accretion rate. This makes in situ formation of “hot Jupiters” by nucleated instability onto the locally formed protoplanetary cores very unlikely.

Results of this study are also important for understanding the ancient atmospheres of terrestrial planets, which must have been significantly depleted.

I am grateful for hospitality to Kavli Institute for Theoretical Physics where part of this work has been done. Useful discussions with Doug Lin, Peter Goldreich, and Bruce Draine are thankfully acknowledged. Author is a Frank and Peggy Taplin Member at the IAS; he is also supported by the W. M. Keck Foundation and NSF grants PHY-007092, PHY99-0794.

APPENDIX

A. SUMMARY OF THE CORE ACCRETION RATES.

Following Rafikov (2003b) we take the core accretion rate to be

$$\dot{M} = \Omega \Sigma_p R_c R_H \theta, \quad (\text{A1})$$

where θ is a parameter set by a particular mode of accretion. In this work we consider the following three important accretion regimes.

First one is characterized by $\theta \approx p \ll 1$ (see definition [11]) and assumes that core accretes planetesimals at a rate set by the core’s geometric cross-section $\sim R_c^2$. This regime is valid when the random epicyclic velocities of planetesimals are larger than the escape speed from the core’s surface and gravitational focusing is weak. We call this regime *slow accretion*. It may occur in planetesimal disks after cores have reached isolation mass by oligarchic growth (Chambers 2001; Goldreich et al. 2004).

Second regime of *intermediate accretion* takes place when random velocities of planetesimals are of the order of shear velocity across the Hill radius of the core ΩR_H . In this case gravitational focusing strongly increases accretion cross-section above its geometric value, and $\theta \approx 1$. Note that this case corresponds to the boundary between the shear- and dispersion-dominated dynamical regimes (Stewart & Ida 2000); it also assumes vertical scaleheight of the planetesimal disk to be $\sim R_H$. This regime may occur during the oligarchic growth of protoplanetary embryos by accretion of large planetesimals (Kokubo & Ida 1998; Rafikov 2003b).

Finally, third regime is realized when random velocities of planetesimals are so low that planetesimal disk is geometrically very thin and essentially two-dimensional. For that one needs random velocities to be smaller than $p^{1/2} \Omega R_H$, which leads to a *rapid accretion* with $\theta \approx p^{-1/2}$. Such dynamically “cold” planetesimal populations can occur even in the presence of massive cores provided that some dissipative process such as gas drag can effectively damp planetesimal velocities. This can happen if fragmentation of large planetesimals in collisions at high velocities (induced by the gravity of protoplanetary cores) is capable of channeling a significant amount of mass initially locked up in large planetesimals into small bodies; see Rafikov (2003a,b) for details of this scenario.

It is likely that each of these accretion regimes can take place during some stage of protoplanetary growth, e.g. starting with intermediate, switching to rapid (or some mixture of rapid and intermediate, depending on the fragmentation timescale, see Rafikov [2003b]), and, possibly, ending with a slow accretion phase. Typical accretion timescale τ_{acc} in each regime is

$$\tau_{acc} \equiv \frac{M_c}{\dot{M}} = \frac{M_c}{\Omega \Sigma_p R_c R_H} \theta^{-1} \approx \left(\frac{M_c}{M_{\oplus}} \right)^{1/3} \begin{cases} 3 \times 10^{10} \text{ yr } a_{10}^3, & \text{slow,} \\ 1.4 \times 10^7 \text{ yr } a_{10}^2, & \text{intermediate,} \\ 3 \times 10^5 \text{ yr } a_{10}^{3/2}, & \text{fast.} \end{cases} \quad (\text{A2})$$

Note that in all three regimes listed here protoplanetary growth proceeds as $M_c \propto \tau^3$, where τ is the time.

B. CALCULATION OF THE ENVELOPE MASS.

As we mentioned in §5.3, because gas density drops exponentially outside R_a , most of the atmospheric mass is confined within this radius and we may replace R_B with R_a in definition (51). Using (28) and (29) for envelopes with radiative interior, and (42), (43), and (45) for envelopes with convective interior we arrive at equation (52), in which Ψ_1 is defined by

$$\Psi_1(u, w, \zeta) \equiv C w \zeta \left(\frac{R_a}{R_B} \right)^{3-\zeta} \int_0^1 z^2 \left(\frac{1}{z} - 1 \right)^\zeta dz, \quad (\text{B1})$$

and for envelopes having radiative interior ($\nabla_0 < \nabla_{ad}$)

$$C = \left(\frac{4\nabla_0}{3} \right)^{1/(1+\alpha)}, \quad u = \xi, \quad w = \nabla_0, \quad \zeta = \frac{1}{\nabla_0} - 1, \quad (\text{B2})$$

while in the case of envelopes having convective interior ($\nabla_0 > \nabla_{ad}$)

$$C = \left(1 - \frac{\nabla_{ad}}{\nabla_0} \right)^{1/(4-\beta)} \left(\frac{4}{3} \frac{\nabla_0 \nabla_{ad}}{\nabla_0 - \nabla_{ad}} \right)^{1/(1+\alpha)}, \quad u = 1, \quad w = \nabla_{ad} \left(1 - \frac{\nabla_{ad}}{\nabla_0} \right)^{1/(4-\beta)}, \quad \zeta = \frac{1}{\gamma - 1}. \quad (\text{B3})$$

Constant ζ is a power law index of density dependence on $1/r$, see equations (28), (29) and (44).

Whenever $\zeta < 3$ integral in (B1) is dominated by the contribution from $r \sim R_a$, in which case M_{env} depends only weakly on the lower integration limit $R_c \ll R_a$ (this is why we set R_c/R_B to 0 in [B1]). Radiative envelopes with constant opacity ($\alpha = \beta = 0$) having $\nabla_0 = 1/4$ and $\zeta = 3$ contain equal amount of mass per every decade in radius; in this case formula (52) still describes the behavior of M_{env} but with $\Psi_1 \sim \ln(R_a/R_c)$ replacing (B1). This can considerably increase the envelope mass since $R_a \gg R_c$. Condition $\zeta < 3$ is always satisfied for dynamically stable convective envelopes which ought to have $\gamma > 4/3$. In the radiative case one needs $\nabla_0 > 1/4$ for $\zeta < 3$; whenever this is not fulfilled the envelope mass is dominated by the innermost part of the atmosphere near R_c , and M_{env} does depend on R_c . We do not consider radiative atmospheres having $\zeta > 3$ deep in the envelope in this study.

C. THERMAL TIMESCALE OF THE ENVELOPE.

We calculate the thermal (or Kelvin-Helmholtz) time for the atmosphere with the outer radiative zone (see §3) and convective interior ($\alpha = 0$, $\beta = 1$, $\nabla_0 = 1/3 > \nabla_{ad}$) with $\gamma = 7/5$. We define thermal time as $\tau_{th} \equiv |E_{tot}|/L$, where $E_{tot} = E_{th} + E_{gr}$ is the total energy contained within R_a — sum of the thermal and gravitational energy of the envelope. It is easy to verify that $E_{th} \sim |E_{gr}|$, meaning that $E_{tot} \sim E_{gr}$ as well. We calculate E_{gr} using (42), (43), and (45):

$$E_{gr} = - \int_{R_c}^{R_a} G \frac{M_c}{r} \times 4\pi\rho(r)r^2 dr$$

$$\approx -4\pi P_0 R_B^3 \left(\frac{R_B}{R_c} \right)^{\frac{3-2\gamma}{\gamma-1}} \left(\frac{4}{3} \frac{\nabla_{ad}\nabla_0}{\nabla_0 - \nabla_{ad}} \frac{R_B\lambda}{R_L^2} \right)^{\frac{1}{1+\alpha}} \frac{\gamma-1}{3-2\gamma} \left(1 - \frac{\nabla_{ad}}{\nabla_0} \right)^{\frac{1}{\nabla_{ad}(4-\beta)}} \nabla_{ad}^{\frac{1}{\gamma-1}}. \quad (C1)$$

This expression is valid for envelopes with convective interiors whenever $\gamma < 3/2$, in which case gravitational energy budget is dominated by the *innermost* part of the envelope, near the core surface (see Harris 1978); this is why E_{gr} in (C1) explicitly depends on R_c . This would be different for atmospheres with convective interiors having $\gamma > 3/2$ — then the energy content is dominated by the *outer* parts of the envelope⁷ and is much smaller than that given by (C1). Energy is also small for envelopes having outer convective zone — their energy is low because of the high interior entropy and associated low density. In a sense, the specific estimate (C1) of E_{gr} sets an upper limit on τ_{th} and the degree of envelope's deviations from the steady state.

Using our adopted values of $\gamma, \nabla_0, \nabla_{ad}$ and luminosity (9), (A1) we find that

$$\tau_{th} \approx \left(\frac{M_c}{M_\oplus} \right)^{5/3} \left(\frac{0.1 \text{ cm}^2 \text{ g}^{-1}}{\kappa_0} \right) \begin{cases} 10^9 \text{ yr } a_{10}^{23/4}, & \text{slow,} \\ 10^3 \text{ yr } a_{10}^{15/4}, & \text{intermediate,} \\ 1 \text{ yr } a_{10}^{11/4}, & \text{fast.} \end{cases} \quad (C2)$$

Comparing this with (A2) one can see that typically $\tau_{th} \ll \tau_{acc}$ justifying our quasi-static approximation to the treatment of the envelope structure. Massive embryos ($M_c \gtrsim 10 M_\oplus$) accreting in the slow regime at $a > 10$ AU should have this condition violated and this may pertain to the development of nucleated instability in the region of giant planets, see §6.2.

At a given location in the nebula the energy stored in the envelope depends only on M_c . Since M_c changes due to planetesimal accretion, envelope energy should also vary in time giving rise to additional luminosity L_g caused by *gas accretion*:

$$L_g \equiv \frac{\partial |E_{tot}|}{\partial \tau} = \frac{\partial |E_{tot}|}{\partial M_c} \dot{M} \sim \frac{|E_{tot}|}{\tau_{acc}}. \quad (C3)$$

Using the definition of τ_{th} we then find that $L_g/L \sim \tau_{th}/\tau_{acc}$. Thus, whenever the quasi-stationary approximation (i.e. $\tau_{th} \ll \tau_{acc}$) is valid, gas accretion luminosity L_g is *small* compared to the core accretion luminosity L , and we can safely neglect it. Mass accretion rate of gas $\dot{M}_{env} \sim \dot{M}(M_{env}/M_c)$ is always smaller than planetesimal mass accretion rate \dot{M} if core is subcritical, i.e. $M_{env} \lesssim M_c$.

D. EFFICIENCY OF CONVECTIVE TRANSPORT.

Our use of equation (8) relies on the assumption of convection so efficient that even infinitesimal deviation of temperature gradient from ∇_{ad} is enough to transport the energy flux produced at the core surface. If this is not the case one has to use mixing-length theory (Kippenhahn & Weigert 1990) to determine the value of ∇ ; here we check if this is ever necessary. Following Kippenhahn & Weigert (1990) we introduce

$$x \equiv \nabla - \nabla_{ad}, \quad W \equiv \nabla_{rad} - \nabla_{ad}, \quad U \equiv \frac{6\sqrt{2}\nabla_{ad} \sigma T^4}{\eta^2 P \kappa \rho} \left(\frac{r^2}{GM_c H_p^3} \right)^{1/2},$$

$$\nabla_{rad} \equiv \frac{3}{16\pi\sigma G} \frac{\kappa L P}{M_c T^4}, \quad H_p \equiv \frac{\partial r}{\partial \ln P}, \quad (D1)$$

⁷ The latter is also true for envelopes with radiative interiors having $\nabla_0 > 1/3$ (which can exist only for $\gamma > 3/2$); most of the energy in the radiative envelopes with $\nabla_0 < 1/3$ is near the core.

where $\eta \sim 1$ is a mixing length parameter, H_p is the pressure scaleheight, and x is a deviation of temperature gradient from ∇_{ad} , which has to be much smaller than unity for (8) to apply. Value of x has to be obtained from the following equation (Kippenhahn & Weigert 1990):

$$\left(\sqrt{x + U^2} - U\right)^3 = \frac{8}{9}U(W - x). \quad (D2)$$

It is clear from this equation that $x \ll 1$ whenever $U \ll 1$, and $UW \ll 1$, since under these assumptions $x \sim (UW)^{2/3}$. Thus, we look for conditions under which $U \ll 1, UW \ll 1$.

In light of the results of §3.3 & 4 we describe the profiles of temperature, density, and pressure in the convective part of envelope by

$$T = T_b \Phi, \quad \rho = \rho_b \Phi^{1/(\gamma-1)}, \quad P = P_b \Phi^{\gamma/(\gamma-1)}, \quad \Phi \equiv 1 + \nabla_{ad} \frac{T_0}{T_b} \left(\frac{R_B}{r} - \frac{R_B}{r_b} \right), \quad (D3)$$

where T_b, ρ_b, P_b are values of temperature, density and pressure at the boundary of the convective zone r_b . In the case of an atmosphere with the outer radiative zone studied in §3.3 one has $r_b = R_a, T_b = T_{conv}, \rho_b = \rho_{conv}, P_b = P_{conv}$, and (D3) reduces to (44). In the case of atmosphere with the outer convective zone $r_b = R_{out}, T_b = T_0, \rho_b = \rho_0, P_b = P_0$ and (D3) yields (48).

One expects deviations of x from zero to be most pronounced in the outer, low density part of the atmosphere which might not be capable of efficient mixing. This corresponds to $r_b \approx R_a$ in the case of outer radiative zone, and $r_b \approx R_B$ in the case of outer convective zone, but in both cases $\Phi(r_b) \approx 1$. In the atmospheres of first type ($R_L^2 \ll R_B \lambda$) we find for $\alpha = 0, \beta = 1, \gamma = 7/5$ using (42), (43), (26) that

$$\begin{aligned} U(R_a) &\approx \frac{6}{\eta^2} \frac{\sigma T_0^4}{c_0 \kappa_0 \rho_0^2 G M_c} \left(\frac{R_L^2}{R_B \lambda} \ln \frac{R_B \lambda}{R_L^2} \right)^2 \\ &\approx \eta^{-2} \left(\frac{M_\oplus}{M_c} \right)^{1/3} \left(\frac{\kappa_0}{0.1 \text{ cm}^2 \text{ g}^{-1}} \right) \begin{cases} 3 \times 10^{-10} a_{10}^{-19/4}, & \text{slow,} \\ 3 \times 10^{-4} a_{10}^{-11/4}, & \text{intermediate,} \\ 0.2 a_{10}^{-7/4}, & \text{fast.} \end{cases} \end{aligned} \quad (D4)$$

Also $\nabla_{rad} \sim \nabla_{ad}$ at $r \approx R_a$, meaning that $W(R_a) \sim 1$ and $UW \sim U(R_a)$. Thus, in the region of giant planets ($a \gtrsim 5$ AU) convection is efficient in the envelopes of protoplanetary cores accreting planetesimals in the slow or intermediate regime. In the case of fast accretion deviations of ∇ from ∇_{ad} at the level of 0.1 – 1 might be expected in the outermost parts of convective zone, at $r \approx R_a$.

In the case of envelopes having outer convective zone ($R_L^2 \gg R_B \lambda$) one finds for $U(R_B)$ expression similar to (D4) but without $R_L^2/R_B \lambda$ terms. Also, $\nabla_{rad} \sim R_L^2/R_B \lambda \gg 1$ at $r = R_B$. As a result,

$$\begin{aligned} U(R_B) &\approx \frac{0.03}{\eta^2} \left(\frac{M_c}{M_\oplus} \right) \left(\frac{0.1 \text{ cm}^2 \text{ g}^{-1}}{\kappa_0} \right) a_1^{15/4}, \\ W(R_B)U(R_B) &\approx 0.5 \frac{L}{\rho_0 c_0^3 R_B^2} \approx \eta^{-2} \left(\frac{M_\oplus}{M_c} \right)^{2/3} \begin{cases} 10^{-4} a_1^{-1/2}, & \text{slow,} \\ 0.03 a_1^{1/2}, & \text{intermediate,} \\ 0.4 a_1, & \text{fast.} \end{cases} \end{aligned} \quad (D5)$$

These estimates demonstrate that in protoplanetary atmospheres around the cores at $a \sim 0.1$ AU, which are likely to have outer convective zones, deviations from purely isentropic convection may only be important for fast and intermediate accretion regimes.

These are the occurrences when the temperature gradient can go superadiabatic at the outer edge of the convection zone and one would get a more accurate estimate of ∇ in the convective regions by actually solving (D2), e.g. see Papaloizou & Terquem (1999). We do not expect this possible superadiabaticity in some localized parts of atmosphere to strongly affect our estimates of M_{env} and M_{cr} since deeper down in the envelope density increases, convection becomes more efficient at transporting the energy, and entropy gradient goes to zero.

REFERENCES

- Brush, S. G. 1990, *Rev. Mod. Phys.*, 62, 43
Chambers, J. E. 2001, *Icarus*, 152, 205
Genda, H. & Abe, Y. 2003, *Icarus*, 164, 149
Genda, H. & Abe, Y. 2004, *Lunar Planet. Sci.*, 35, #1518
Goldreich, P., Lithwick, Y., & Sari, R. 2004, astro-ph/0404240
D'Angelo, G., Henning, T., & Kley, W. 2002, *A&A*, 385, 647
D'Angelo, G., Kley, W., & Henning, T. 2003, *ApJ*, 586, 540
Draine, B. T. 2003, *ARA&A*, 41, 241
Harris, A. W. 1978, *Lunar Planet. Sci.*, 9, 459
Hayashi, C., Nakazawa, K., & Mizuno, H. 1979, *Earth & Plan. Sci. Lett.*, 43, 22
Ikoma, M., Emori, H., & Nakazawa, K. 2001, *ApJ*, 553, 999
Ikoma, M., Nakazawa, K., & Emori, H. 2000, *ApJ*, 537, 1013
Inaba, S. & Ikoma, M. 2003, *A&A*, 410, 711
Kippenhahn, R. & Weigert, A. *Stellar Structure and Evolution*; Springer-Verlag, 1990
Kokubo, E. & Ida, S. 1998, *Icarus*, 131, 171
Lin, D. N. C. & Papaloizou, J. C. B. 1993, in *Protostars and planets III*, 749
Mizuno, H., Nakazawa, K., & Hayashi, C. 1978, *Progr. Theor. Phys.*, 60, 699
Mizuno, H. 1980, *Progr. Theor. Phys.*, 64, 544
Nakazawa, K., Mizuno, H., Sekiya, M., & Hayashi, C. 1985, *J. Geomag. Geoelectr.*, 37, 781

- Papaloizou, J. C. B. & Terquem, C. 1999, ApJ, 521, 823
- Perri, F. & Cameron, A. G. W. 1974, Icarus, 22, 416
- Pollack, J. B., Hubickyj, O., Bodenheimer, P., Lissauer, J. J., Podolak, M., & Greenzweig, Y. 1996, Icarus, 124, 62
- Rafikov, R. R. 2002, ApJ, 572, 566
- Rafikov, R. R. 2003a, astro-ph/0310392
- Rafikov, R. R. 2003b, submitted to AJ, astro-ph/0311440
- Safronov, V. S. 1969, *Evolution of the Protoplanetary Cloud and Formation of the Earth and Planets*; Nauka, Moscow
- Sasaki, S. 1989, A&A, 215, 177
- Saumon, D. & Guillot, T. 2004, astro-ph/0403393
- Stewart, G. R. & Ida, S. 2000, Icarus, 143, 28
- Stevenson, D. J. 1982, Planet. Space Sci., 30, 755
- Stevenson, D. J. 1984, Lunar and Planetary Science Conference XV, 822
- Tassoul, J.-L. *Theory of Rotating Stars*; Princeton University Press, 1978
- Wuchterl, G. 1993, Icarus, 106, 323